Recurrent early Paleozoic rifting in the Northern Gondwana margin: Evidence from correlation of metabasalts across the Saxothuringian Zone of the Bohemian Massif

Václav Kachlík, Vladislav Rapprich, John M. Hora, Ondřej Pour, Zuzana Čvančarová, Ottomar Krentz, Quentin Crowley, Tomáš Magna

PII: S0012-8252(26)00165-0

DOI: https://doi.org/10.1016/j.earscirev.2026.105554

Reference: EARTH 105554

To appear in: *Earth-Science Reviews*

Received date: 19 February 2026

Revised date: 19 May 2026

Accepted date: 23 May 2026

Recurrent early Paleozoic rifting in the Northern Gondwana margin: Evidence from correlation of metabasalts across the Saxothuringian Zone of the Bohemian Massif

Václav Kachlík[1,*], Vladislav Rapprich[2], John M. Hora[2], Ondřej Pour[2], Zuzana Čvančarová[2], Ottomar Krentz[3], Quentin Crowley[4], Tomáš Magna[2]

[1] Institute of Geology and Paleontology, Faculty of Science, Charles University, Albertov 6, CZ-128 43 Prague 2, Czech Republic

[2] Czech Geological Survey, Klárov 131/3, CZ-118 00 Prague 1, Czech Republic

[3] Am Rosenhain 5, D-09627 Bobritzch-Hilbersdorf, Germany

[4] School of Natural Sciences, Faculty of Science, Technology, Engineering & Mathematics, Trinity College Dublin, Dublin 2, D02 PN40, Ireland

* Corresponding author. Email: vaclav.kachlik@natur.cuni.cz

For consideration in ***Earth-Science Reviews***

Word count abstract:	246
Word count main text:	9548
Characters w/spaces (abstract, main text, acknowledgements):	67887
Figures:	10
Tables:	2

Abstract

Geodynamic causes of the Rhenohercynian basin opening and Devonian–early Carboniferous rifting within the Saxothuringian Zone of northern peri-Gondwana and the Variscan basement of the Alps remain unresolved. Interpretations with varying numbers of oceanic tracts formed during Paleozoic fragmentation of Peri-Gondwana exist, heretofore without a comprehensive survey linking Rheic rift-related segments. A review of existing data, combined with new evidence from three separate Rheic/Saxothuringian rift system segments in the Bohemian Massif, informs a new three-stage model of their Paleozoic evolution:

(1) Late Cambrian–early Ordovician (~505–470 Ma) rifting accompanying back-arc extension along the northern Gondwana margin, was coeval with Rheic Ocean opening between Avalonia and Saxothuringia. Initial bimodal felsic and mafic OIB-like magmas transitioned through T-MORB to MORB-like basalts, common in NE Saxothuringia.

(2) Subordinate Silurian–early Devonian (~430–410 Ma) extension of both Saxothuringian and Teplá-Barrandian basement was possibly linked to closure of Iapetus Ocean and accretion of microcontinental fragments to Laurentia. Proximal to the Münchberg Massif, this manifests as strongly alkaline OIB-type volcanism, whereas more tholeiitic magmas prevail in the adjacent Teplá-Barrandian Unit.

(3) Middle-Devonian–early Carboniferous (390–340 Ma) extension produced the most voluminous magmatism, similarly progressing from early bimodal alkaline rhyolite and OIB-type basalts to MORB-like compositions proximal to the Saxothuringian ocean tract. This rift-related volcanism overlaps in chemistry and time with alkaline volcanism of the SE edge of Avalonia, grading into of the Rheic/Rhenohercynian oceanic basalts. Late Devonian/early Carboniferous closure of this ocean is linked to cessation of extension, its shift back to the Gondwana margin and opening of the Paleotethys Ocean.

Keywords: Saxothuringian, rifting, Gondwana, Paleozoic volcanism, geochemistry, geochronology, radiogenic isotopes

1. Introduction

The beginning of the Paleozoic era is marked by significant re-arrangement of continents. During the Cambrian, the Neoproterozoic–Cambrian Avalonian–Cadomian Belt (Murphy and Nance, 1989) began to separate from the Gondwana mega-continent (Nance et al., 2022) forming a belt of (micro-)continents accreted mostly to the margins of Laurentia–Baltica. Transition from the Cadomian (Neoproterozoic) accretionary orogeny to Cambro–Ordovician rifting and opening of the Rheic Ocean was a multi-step process. Transformation of the Gondwana periphery from active to passive continental margin (Linneman et. al., 2007; Murphy et al., 2010) was accompanied by a shift from Cambrian calc-alkaline (García-Arias et al., 2024) to transitional alkaline ocean island basalt (OIB) magmatism (Crowley et al., 2000), associated with plume-initiated intracontinental rift-related volcanism. Opening of the Rheic Ocean and separation of Avalonia in the Early Ordovician was likely caused by the accretion of the Ganderia micro-continent to Laurentia (e.g., Kroner and Romer, 2013; Linnemann et al., 2007; Murphy et al., 2009, 2010; Nance et al., 2008; Romer and Hahne, 2010). Re-activated rifting of the passive margin of Gondwana since the Ordovician initiated sedimentation in extensional basins; these sedimentary successions are preserved across the Variscan belt (e.g., Kraft et al., 2023; Linnemann, 2004; Patočka and Štorch, 2004). Opening of the rift was associated with predominantly mafic magmatism (submarine volcanism) progressing from OIB to mid-ocean ridge basalt (MORB)-like (Crowley et al., 2000; Tasáryová et al., 2018). A third stage of rifting resulted in either formation of Devonian to early Carboniferous Rhenohercynian Ocean basins in the rifted southern part of the Avalonian margin (Floyd et al., 1990; Franke, 2007) or a back-arc to the N branch of the still existing Rheic Ocean (Nesbor, 2025; Zeh et al., 2002). Alternatively, the Rhenohercynian Ocean tract might have originated by intra-arc or back-arc extension, associated with southward subduction of southern margin of the Rheic Ocean beneath the Gondwana derived part of Mid-German Crystalline High (Franke et al., 2017; Franke and Żelaźniewicz, 2023).

Radiometric dating and geochemistry of bimodal volcanic and metavolcanic rocks and metaophiolites situated within or between Gondwana-derived ribbon continents (for example between Saxothuringian/Teplá–Barrandian/Brunovistulian/Moldanubian domains) indicate that the mid- to late-Devonian to the early Carboniferous was associated with pronounced extension and limited ocean crust-forming processes within the future Variscan orogen of Central and Western Europe (Franke and Żelaźniewicz, 2023; Höhn et al., 2018; Koglin et al., 2017; Kachlík and Kozdroj, 2001). Opening of the Rhenohercynian basin and Middle Devonian to early Carboniferous rifting within the Saxothuringian Zone and in the Variscan basement of the Alps, and its geodynamic causes during the onset of overall Variscan compression still remain controversial (Franke, 2024).

The above-outlined complex tectonic situation gives rise to many alternative interpretations regarding the number of oceanic tracts which might have formed during the Paleozoic fragmentation of the Peri-Gondwana: (i) Rheic Ocean was fully opened without branching (Kroner and Romer, 2013); (ii) at least two branches of the Rheic Ocean – so-called Saxothuringian and Moldanubian (Central European, Gföhl oceans) were developed (e.g., Franke et al., 2017; Franke and Żelaźniewicz, 2023, and references therein for details); (iii) sediments were deposited on a hyperextended shelf formed by the Cadomian basement (Žák and Sláma, 2018; Žák et al., 2023b); (iv) ribbon continents were not significantly separated from the parental Gondwana Mainland (Kroner et al., 2007).

A comprehensive study connecting the occurrences of Rheic rift-related mafic rocks is largely missing. We aim to improve the understanding of the timing and potential causes of Rheic rifting during coeval stages of Variscan collision, by reviewing the existing data on Ordovician to Devonian mafic volcanic rocks of the Münchberg Massif, Krkonoše–Jizera

Crystalline Units and Prague Basin, paralleled by a detailed lithostratigraphic, petrographic, geochemical, geochronological and radiogenic isotope (Sr, Nd, Pb) survey of mafic volcanic rocks from Frankenberg, Elbetalschiefergebirge and Ještěd Mts. These new results, combined with published data, identify potential mantle sources of Paleozoic volcanism, their temporal difference and/or evolution during the individual stages of Rheic rifting, evaluate the role of mantle plumes for individual stages of rifting or continental fragmentation, and constrain differentiation of mantle magmas and their possible contamination with crustal material.

2. Geological setting

The Saxothuringian Zone of the European Variscan orogenic belt is a >100 km wide and ~1,000 km long crustal segment, comprising the N and NW part of the Bohemian Massif (**Fig. 1**) and is thought to have been derived from the Peri-Gondwanan margin at the beginning of the Ordovician concomitant with opening of the Rheic Ocean or, possibly, its branches (Linnemann et al., 2008). In the southeast, the Saxothuringian ribbon continents plunge below the Teplá–Barrandian Unit (TBU) supracrustal block. The Mariánské Lázně Complex, interpreted as a metaophiolite relic, straddles the TBU boundary and traces the Teplá (Saxothuringian) suture after the Saxothuringian branch of the Rheic Ocean (Behr et al., 1980; Franke, 1989a; Kachlík, 1994). Part of the Paleozoic oceanic crust consists of allochthonous crystalline sheets thrust from the Teplá suture to the NW onto the Saxothuringian parautochthon (Behr et al., 1980; Martínez Catalán et al., 2020; Collett et al., 2018; Franke, 1989a).

The Saxothuringian crust is composed of Cadomian basement, deformed and weakly metamorphosed during the final stages of the Cadomian orogeny (ca. 570–540 Ma; Dörr et al., 2004; Linnemann et al., 2000, 2014). This basement is overlain by a thick Paleozoic sequence of folded and variably metamorphosed volcanosedimentary sequence of the Cambrian to early Carboniferous age. The Neoproterozoic basement together with Paleozoic onlap sequences were strongly folded and metamorphosed during several stages of the Variscan orogeny starting with Devonian closure of oceanic tracts, through early Carboniferous continental collision of Avalonia with Saxothuringia and the TBU block, forming the Variscan–Alleghanian orogen (Martínez Catalán et al., 2020, 2021; Franke et al., 2017; Franke and Żelaźniewicz, 2023; Schulmann et al., 2022). Folded early Paleozoic sequences are unconformably overlain by late Carboniferous to Permian continental molasse and associated volcanic rocks.

The Saxothuringian Zone may be divided into four lithotectonic units: (i) the sub-parautochthon of the Saxonian Granulite Massif which forms an extrusive antiformal diapiric structure (Rötzler and Timmerman, 2021); (ii) Saxothuringian autochthon comprising weakly deformed and metamorphosed Cadomian basement unconformably overlain by Cambrian to Devonian siliciclastic sequences of the Saxothuringian passive margin, covered by Variscan distal flysch sediments (Linnemann et al., 2008a); (iii) Saxoturingian parautochthon to lower allochthon (sensu Martínez Catalán et al., 2021) formed by (U)HP–UHT folded crystalline nappes in the Krušné hory/Erzgebirge Mts. and in the Ohře (Eger) Crystalline Complex, which follow the Teplá Suture (e.g., Massonne and Bautsch, 2004; Schmädicke et al., 2018; Willner et al., 2000); (iv) Saxothuringian uppermost allochthons occurring in tectonic klippen such as Münchberg Massif, Zone Erbendorf–Vohenstraus, Wildenfels, Frankenberg, Elbtaschiefergebirge and western part of the Ještěd Mts., and possibly Góry Sowie Mts. (Franke et. al., 1993; O'Brien et al., 1997; Franke and Żelaźniewicz, 2023).

In this study, we sampled metabasaltic rocks from three separate segments of the Rheic/Saxothuringian rift system (**Fig. 2a**). (a) Frankenberg klippe (Becker, 1928) is a narrow NNE–SSW trending, synformal stack of tectonic slices, with variable protolith ages, provenance and metamorphic evolution, located between the Saxonian Granulite Massif on the west and Krušné hory/Erzgebirge Mts. antiform in the east (**Fig. 2b**). According to Gehmlich et al. (2001) and Kurze (1993) the Frankenberg klippe consists of, from bottom to top, of a sliver of Viséan flysch, Ordovician sandstones, Silurian black shales containing cherts and Devonian greenish tuffitic and graphitic slates and felsic volcanic rocks dated at 357 ± 2 Ma (Gehmlich et al., 2001). This unit also contains well-preserved pillow lavas with associated hyaloclastites and metadolerite feeding dyke, exposed in the Seifersdorf quarry in the NE part of the Frankenberg klippe (**Fig. 2b**).

(b) The Elbtalschiefergebirge is a NW–SE trending imbricated belt formed by Ordovician to early Carboniferous volcanosedimentary sequences, dividing the Lusatian block and Krušné hory/Erzgebirge Mts. antiform, delimited by the Mid-Saxonian Fault on the southwest and the Weesenstein Fault on the northeast (**Fig. 2c**). The Elbtalschiefergebirge unit consists, from bottom to top, of several fault-bounded slices in greenschist facies grade: (i) Ordovician slates to phyllites, chlorite gneiss and metavolcanics (so called „Phyllitic unit" or Mühbach-Nossen Group after Alexowsky et al., 1997) intruded by 485 Ma tourmaline granite (Hofmann et al., 2009), (ii) a Devonian volcanosedimentary unit with sheared felsic volcanic rocks dated at 369 ± 5 Ma (Hofmann et al., 2009), (iii) a Silurian to Late Devonian volcanosedimentary unit rich in amygdaloidal lavas, limestones, metabasalts and tuffitic phyllites (diabase–marl series, Thuringian facies after Kurze (1993), (iv) Late Ordovician to early Carboniferous sequence of sandstones, deep-water silicic shales (chert series, Bavarian facies after Kurze (1993), and (v) probably Middle- to Late-Devonian volcanosedimentary facies, rich in pillow lavas, volcanoclastics and shallow-water carbonates, often with contact metamorphic overprint (so called Donnerberg- and Bahre-Formation after Alexowsky et al., 1997). The Ediacaran Weesenstein Group, consisting of greywackes, shales with intercalations of glaciomarine conglomerates with pebbles of Ediacaran granite overthrust Paleozoic units of the Elbtalschiefergebirge is typically not considered a part of the Elbtalschiefergebirge unit.

(c) The Ještěd Mts. Unit crops out in the NW part of the Krkonoše–Jizera Mts. Crystalline Unit (NE part of the Bohemian Massif; **Fig. 2d**). On the SW, it is bounded by Lusatian overthrust to Cretaceous marine sediments or to the underlying Permo-Carboniferous continental molassic sediments. It is delimited on the NE by the Machnín fault against the Variscan (320–312 Ma) Krkonoše–Jizera Pluton (Žák et al., 2013). From NW to SE the following fault-bounded lithotectonic units can be defined: (i) Cadomian basement, built of ~532 Ma cataclastically deformed granodiorites (Bialek et al., 2014) and greywackes intruded by late Cambrian orthogneisses; (ii) sequence of Cambrian (?) to Ordovician phyllites, with quartzite, Silurian black shales, phyllites with fossiliferous late Silurian, and Middle to Late Devonian fossiliferous limestones (Chlupáč and Hladil, 1992); (iii) This parautochthonous sequence is in its SW part overthrust by a Middle Devonian to early Carboniferous volcano-sedimentary sequence comprising both felsic and mafic volcanic rocks, nodular limestones, black shales and tuffitic phyllites (**Fig. 2d**). This sequence is conformably overlain by a sequence of Tournaisian to Viséan flysch. Sediments of these units may be correlated with Bavaria Facies of surrounding of Uppermost allochthons in Frankenwald and Thuringia.

3. Samples and methods

We collected 15 new samples of weakly metamorphosed basaltic rocks representing three spatially separated areas with occurrences of Devonian basaltic lithologies (**Fig. 2**; Electronic Supplementary Material 1). The Frankenberg tectonic klippe was sampled at the Seifersdorf quarry (Germany; **Fig. 2b**): three Devonian pillow lavas (MLC22/039B,C,D) and one sample of a dolerite conduit (MLC22/039A) closely associated with the pillow lavas. Five samples of

Devonian to early Carboniferous metabasites were collected from boreholes VRT_D_1 in the Bahre-Formation and VRT_D_2 from the diabase-marl series (after Kurze 1993) in the Elbtalschiefergebirge south of Pirna (Germany; **Fig. 2c**). The Weesenstein Fault, part of the West Lusatian Fault zone, was intercepted at a depth of 52.9–59.4 m in drill hole VRT_D_1 in the Bahre-Formation. Ediacaran schists and metagreywackes overthrust on Devonian metabasalts that alternate with dark-grey (organic matter-rich) phyllitic shales (**Fig. 3**). Carbonate bodies, commonly banded and containing mafic volcanoclastic layers metamophorphosed in greenschist to epidote amphibolite facies, were encountered at depths of 149–165 m and 172–199 m, respectively. Layers of abundant amygdales (up to 1 cm in diameter) were documented at the bottom of several metabasalt bodies (e.g., at ca. 130 and 200 m). Thin intercalation of biotite–cordierite hornfels was sampled at depth 226 m. Borehole VRT_D_2 in the Late Devonian diabase-marl series cuts the sequence of alternating basaltic tuffs, marbles and metabasalts and phyllitic shales. A doleritic metabasalt dyke was sampled at a depth of 201 m. Finally, four metabasite samples were collected from the Late Devonian to Lower Carboniferous Jítrava Group, Ještěd Mts. (Czech Republic), representing an allochthonous relic preserved in the overburden of the volcanosedimentary parautochthonous complex of Cambrian to Devonian age (**Fig. 2d**) correlatable with Thuringian Facies Realm. Sample JG13 is an amygdaloidal lava, samples JG-9 and ZB443 are metadolerite dykes within dark black, finely laminated and often silicified phyllites of Late Devonian to early Carboniferous age, and sample JG260 is a dolerite dyke cutting the sheared Ordovician orthogneisses.

For detailed description of methodological and instrumental approach taken for petrography, mineral and bulk rock chemistry, Sr, Nd, and Pb isotopic systematics, and U–Pb geochronology see ESM 2, ESM 3, and ESM 4.

4. Results

4.1 Petrography and mineral chemistry

Detailed petrography is presented in ESM 2. Below, we describe the main petrographic features and provide mineral phase classifications (mineral chemistry data are available in ESM3).

Basaltic rocks of the Frankenberg tectonic klippe are dominated by originally glassy pillow lavas (samples MLC22/039B,C,D) with intersertal texture, flow-oriented magmatic phases and amygdales up to ~4.5 mm large (**Fig. 4a**). Mineralogy and mineral chemistry of these samples is better demonstrated by sample MLC22/039A (**Fig. 4b**) representing a feeding dyke cross-cutting the pillow lavas. It is a fine-grained rock consisting of subhedral to euhedral phenocrysts of clinopyroxene which falls into the diopside field in the quadrilateral classification diagram (Morimoto, 1988; **Fig. 5a**), but low Ca *apfu (atoms per formula units)* values (<0.9) indicate augite character (**Fig. 5b**; Rapprich 2005). Clinopyroxene in these lavas is significantly enriched in Ti (up to 0.13 *apfu*; **Fig. 5c**) indicative of alkaline tendency of source magma and low-pressure crystallization (e.g., Rapprich et al., 2017; Tracy and Robinson, 1977). Randomly oriented original plagioclase experienced albitization (**Fig. 4e**) reflecting reaction between lavas and seawater and superposed greenschist facies metamorphism. Manganese-rich ilmenite (up to 0.3 *apfu* MnO; **Fig. 5d**) forms long prismatic subhedral microliths in the flow-oriented matrix and anhedral grains occurring in secondary chlorite replacing glassy matrix. Titanite and apatite are common accessory phases.

All Elbetalschiefergebirge samples from boreholes VRT_D_1 and VRT_D_2 are variably deformed metadolerites with typical doleritic textures (**Fig. 4c,d**), where euhedral to subhedral wide plagioclase laths enclose anhedral pyroxene, here mostly replaced by uralite. Metadolerites from different depths differ in grain size of feldspar, hornblende and ilmenite phenocrysts, and intensity of deformation and recrystallization of primary phases during regional shearing, followed by contact metamorphism from a hypothetical Variscan plutonic body.

Sample VRT_D_1/187 is a fine-grained metadolerite or chilled margin of a metadolerite sill/dyke (**Fig. 4c**). It consists of euhedral to subhedral, mostly twinned narrow laths of albite enclosing yellow greenish amphibole and fine-grained anhedral ilmenite inclusions in amphibole and plagioclase. Epidote, titanite and apatite are common accessory phases. Medium- to coarse-grained metadolerites are more common, represented by samples VRT_D_1/82 (**Fig. 4d**), VRT_D_1/135, VRT_D_1/251 and VRT_D_2/201. Some of these samples underwent cataclastic fragmentation of feldspar, which is to some extent dynamically recrystallized along the margins. Sample VRT_D_1/125.7 is texturally distinct strongly ductile-deformed metadolerite with a well-developed metamorphic foliation. Yellow-green to pale green former uralitized pyroxene is completely replaced by variably rotated actinolite porphyroclasts (**Fig. 4e**), which are surrounded by fine-grained matrix composed of fibrous magnesiohornblende and cummingtonite, and partly albitized plagioclase with accessory K-feldspar. Larger feldspar phenocrysts are not preserved. Large ilmenite grains are broken to anhedral grains forming aggregates mostly parallel to dominant foliation, and are wrapped around hornblende porphyroclasts. Other common accessory phases are rutile, titanite and apatite. Clinopyroxene was preserved solely in sample VRT_D_2/201, having augitic composition (**Fig. 5a,b**). Despite slightly elevated Ti content (up to 0.05 *apfu*; **Fig. 5c**), its concentration does not reach the values observed in Frankenberg klippe. On the other hand, amphibole is present in all samples from the Elbtalschiefergebirge. Its variable Mg# (Mg/[Mg+Fe] = 0.2–0.8 *apfu*; **Fig. 5e**) likely reflects bulk-rock compositional differentiation. A large range in amphibole Si contents is observed within individual samples, generally with higher Si (actinolite) cores and lower Si (ferro- or magnesio-hornblende) rims (**Fig. 5e**).

Plagioclase is albitized to some extent, but primary labradorite to andesine composition is preserved in larger porphyroclasts (**Fig. 5f**). Strong deformation of ilmenite is associated with its recrystallization and compositional shift towards low Mn and elevated Mg contents (up to 0.01 *apfu*; **Fig. 5d**).

Similar petrography was documented in the metadolerite sample VRT_D_1/81, comprising thick and commonly broken plagioclase laths (An_{49-57}; **Fig. 5f**), yellow-green to pale green hornblende, filling space between omnidirectional plagioclase laths, subhedral magmatic ilmenite enclosing both plagioclase and amphibole phenocrysts and relic grains of clinopyroxene. Despite these similarities, significantly distinct composition of clinopyroxene (diopside to hedenbergite; **Fig. 5a**) depleted of Ti (**Fig. 5c**) points to a distinct source of parental magma.

The Ještěd Mts. samples represent late Devonian to early Carboniferous fine-grained amygdaloidal lavas and their feeding conduits. These volcanic rocks are in contact with black shales, nodular limestones and fine-grained metaaleurites paleontologically dated to the Late Devonian to early Carboniferous (Chlupáč, 1993; Chlupáč and Hladil, 1992). Sample JG13 is a ductile-deformed and greenschist facies recrystallized amygdaloidal lava of basaltic composition. Randomly oriented laths of albitized plagioclase are enclosed together with accessory ilmenite in chlorite matrix, possibly replacing original glass (**Fig. 4f**). Vesicles are irregular and filled with chlorite and calcite. Metadolerites ZB-443, JG-9 and JG-260 are medium-grained, weakly porphyritic, with typical doleritic texture, where euhedral albitized and often saussuritized plagioclase (**Fig. 4g,h**) encloses strongly fractured clinopyroxene. Some partly corroded clinopyroxene phenocrysts enclose euhedral plagioclase laths and skeletal ilmenite crystals (**Fig. 4h**). Primary magmatic ilmenite is fragmented and overgrown, locally almost completely replaced, by titanite. Clinopyroxene has similar composition to other studied metadolerite samples, classified as augite (**Fig. 5a**), with only weakly elevated

Ti contents (0.02–0.05 *apfu*; **Fig. 5c**) reflecting the intrusive character of these rocks. Clinopyroxene usually is variably replaced by pale actinolite (**Fig. 5e**) and chlorite. Matrix of these samples consists of small, mostly twinned albitized plagioclase (**Fig. 5f**) laths accompanied with small subhedral ilmenite grains and secondary phases such as epidote, chlorite, calcite and titanite. Long prismatic to needle-like apatite and K-feldspar are typical accessory phases.

4.2. Bulk rock geochemistry

Major and trace element compositions of samples from this study are listed in **Table 1**, whereas analytical methods used for bulk rock major element, trace element, and Sr, Nd and Pb isotopic ratio determinations are described in ESM 4. In the TAS classification diagram (Le Maitre et al., 2005; **Fig. 6a**) almost all samples from all three studied areas form a tight cluster in the field of basalts with transition to trachybasalts; only sample VRT_D_1/135 departs towards more differentiated basaltic andesite composition. Likewise, the classification of Pearce and Wyman (1996) based on immobile trace elements Zr/Ti vs. Nb/Y (**Fig. 6b**) replicates homogeneous clustering of basalts from this study. They overlap with Devonian dykes of the Jizera Mts. Devonian basalts of the Münchberg block and Silurian basalts of the Prague basin, all plotting within the alkali basalt field with transition to subalkaline basalts with Nb/Y <1.7, whereas Ordovician and Silurian volcanic rocks of the Münchberg klippe display well-constrained alkaline (Nb/Y >1.7) differentiation trend extending to tephriphonolites. Subalkaline character of sample VRT_D_1/81 is confirmed by bulk-rock chemistry (**Fig. 6b**).

Classification at the alkaline/subalkaline boundary is consistent with the observed petrography because dominant basic plagioclase, indicative of tholeiitic affinity at low silica content, is associated with subordinate augite, common in alkali basalts. The transitional nature of this trend can additionally be tested using tectonic diagrams. Uniformly high Nb/La ratios >0.6 (**Fig. 6c**) point to the origin via decompression melting in the discrimination diagram by Hollocher et al., (2012), but the entire data set, including published values, appears to be subdivided into two subgroups according to their La/Yb ratio. This may reflect the degree of partial melting with Ordovician and Silurian volcanic rocks of the Münchberg block displaying notably elevated La/Yb = 14–30 compared to samples from this study and other localities, having La/Yb < 14 (with several outliers; **Fig. 6c**). Here, sample VRT_D_1/81 plots into the field of continental arcs with low Nb/La = 0.29 and La/Yb = 3.25. Likewise, using Th–Hf/3–Nb/16 discrimination plot of Wood (1980; **Fig. 6d**), Ordovician and Silurian volcanic rocks of the Münchberg block have a typical signature of intraplate alkaline rocks related to a mantle plume whereas all other groups, including new samples from this study, depart towards E-MORB- or within plate-like composition. The somewhat anomalous nature of sample VRT_D_1/81 is evidenced by contrastingly low Th and Nb concentrations. Despite low Hf content (0.54 ppm), strong depletion in Th and Nb shifts this sample towards the Hf end of the diagram and places sample VRT_D_1/81 into the N-MORB field (**Fig. 6d**).

Chondrite-normalized REE patterns (**Fig. 7a**) indicate variable degrees of partial melting, most likely reflecting distinctively different stages of transition from a continental rift (with OIB-like magmas) to early oceanic rift (MORB-like magmas). Despite higher REE contents in Devonian volcanic rocks compared to Silurian basalts of the Prague Basin (Barrandian) – Tasáryová et al. (2018), they all show similar REE slopes (La_N/Yb_N = 3.7–12.7 for the new data, 3.2–14 including published data). Most samples have La_N/Yb_N <9.3, with a few exceeding this value. Shallower REE slopes differentiate Devonian basalts from steeper trends observed for Ordovician and Silurian volcanic rocks of the Münchberg block (La_N/Yb_N = 9.9–21; **Fig. 7b**). This points to lower degrees of partial melting recorded in the latter samples. Very low REE contents of sample VRT_D_1/81 (ΣREE = 34.5 ppm versus 105–316 ppm for all other samples analyzed here) paralleled with a rather flat REE pattern (La_N/Yb_N = 2.2; **Fig. 7a**) indicate derivation of this sample from strongly depleted mantle source via high-degree partial melting whereas positive Eu anomaly (Eu/Eu* = 1.13) points to some amount of plagioclase accumulation.

The incompatible trace element patterns (**Fig. 7c–f**) also support a close genetic relationship between samples from this study and Devonian volcanic rocks of the Münchberg block (**Fig. 7c,e**). Ordovician and Silurian volcanic rocks of the Münchberg block display generally higher contents of incompatible elements, particularly "high field strength elements (HFSE)" (**Fig. 7d,f**). High variability and, for submarine lavas, also strong enrichments in highly mobile lithophile elements (Cs = 0.15–56 ppm, Rb = 2.5–61 ppm, Ba = 73–614 ppm) may result from interactions of lavas and high-level intrusions with seawater or hydrous fluids percolating in the sub-seafloor environment.

4.3. Zircon U-Pb geochronology

Sample ZB-520 (greenschist facies-sheared rhyolite - porphyroid, see ESM 2 for a detailed description) contains mostly long prismatic to stubby (60–250 μm), mostly idiomorphic zircon grains preserving primary magmatic oscillatory zoning patterns, but probably inherited older rounded brownish zircons also occur. The calculated $^{206}Pb/^{238}U$ ages range from ~460 Ma to 385 Ma (ESM 5), but the best-defined age cluster yields a concordia age of 386.8 ± 1.7 Ma (**Fig. 8**), interpreted here as the crystallization age of the felsic source magma. Several zircon grains with ages of up to 420 Ma show disturbed (discordant) ages indicative of Pb loss; these may represent inherited zircons or older cores. The new U–Pb age from this study slightly extends the paleontologically-evidenced age of Jítrava Group (Galle and Chlupáč,

1976) to Middle Devonian (Givetian), which is also indicated by fossil evidence from the autochthonous (Thuringian facies domain) from the central and southeastern part of the Ještěd Mts. and by the unpublished 391 ± 2.6 Ma zircon U–Pb age of a porphyroid sample from the eastern part of the Ještěd Mts.

4.4 Isotope systematics of Sr, Nd and Pb

The Sr, Nd and Pb isotope compositions of samples from this study are listed in **Table 2** and plotted in **Fig. 9**. These new data are then compared with published Cambro-Ordovician, Silurian and Devonian (meta)volcanic rocks, sills and dyke samples from different parts of the Saxothuringian Basin (Lucassen et al.,2025), and Silurian volcanic rocks, associated sills and dykes from the Prague Basin (Tasáryová et al., 2018). The initial Nd isotopic compositions recalculated to 387 Ma range from 0.5122 to 0.5124 (**Fig. 9a**) with corresponding ε_{Nd} values from +4.38 to +6.11 (**Fig. 9c**), and calculated T_{DM} ages varying from 0.702 to 1.208 Ga (ESM 6). Most samples plot in the field of OIB alkaline basalts, except for pillow lava samples VRT_D_1 and VRT_D_2, for which Sr isotope compositions are probably shifted to lower or slightly higher value at a given ε_{Nd}. Because Sr is highly mobile during greenschist facies metamorphism and secondary alteration is evidenced by calcite-filled amygdales, the primary Sr isotopic ratios were likely influenced by reaction of lava with seawater and hydrothermal fluids. The most depleted source with $\varepsilon_{Nd} > 6$ is found for pillow lava (MLC22/039B,C), showing only a limited open-system fractionation, in contrast to amygdaloidal lavas, and especially dolerite sills and dykes in 1/Nd vs ε_{Nd} and La/Yb vs ε_{Nd} plots (not shown). The ε_{Nd} values of metadolerites vary from +5.94 in cpx-bearing metadolerite MLC22/039A from the Seifersdorf quarry to +3.3 in uralitized metadolerites from the Elbtalschiefergebirge (VRT_D_1/187). Strong positive correlations between La/Yb vs. Sm/Yb and Nb/Yb vs.

Th/Yb (not shown) indicate that the variation of ε_{Nd} values may reflect mixing between OIB and P-MORB melts, generated at different mantle depths and by variable degrees of melting.

The $^{87}Sr/^{86}Sr_{(i)}$ values range from 0.7038 to 0.7056 (**Table 2; Fig. 9c**) and two groups can be identified. Metadolerites show generally lower values between 0.7038 and 0.7049, whilst $^{87}Sr/^{86}Sr_{(i)}$ values of pillow and amygdaloidal lavas range from 0.7049 to 0.7056. They are negatively correlated with $\varepsilon_{Nd(i)}$ values. The less radiogenic Sr group broadly follows the EM-II trend whereas samples with slightly more radiogenic Sr isotopic compositions tend towards the EM-I composition according to Kostitsyn (2007).

The $^{206}Pb/^{204}Pb$ vs. $^{207}Pb/^{204}Pb$ plot distinguishes between the two above-mentioned groups (**Fig. 9b**). The $^{207}Pb/^{204}Pb$ ratios of lavas range between 15.61 and 15.64, while those of metadolerites range from 15.64 to 15.75. The $^{208}Pb/^{204}Pb$ ratios are lower and uniform for pillow lavas (**Fig. 9b**), while $^{206}Pb/^{204}Pb$ increases up to 21.39. The ratios for lavas fall into the field of HIMU and OIB, and metadolerites tend to shift to source HIMU ($^{206}Pb/^{204}Pb$ >20). This means that metadolerites and lavas have different sources influenced by subduction processes in the past, or they were increasingly influenced by reaction of fluids during Variscan greenschist facies metamorphism which resulted in Pb loss from the rocks and increased the U/Pb ratio.

5. Discussion

5.1 Age correlations of metavolcanic rocks within the Saxothuringian Zone

The ages of pillow lavas exposed in the Seifersdorf quarry (part of the Frankenberg klippe), have not yet been accurately determined paleontologically or using conventional geochronology. The Middle–Late Devonian age of the lavas is only indirectly inferred from their stratigraphic position under the Lower to Middle Mississippian flysch, which contains fragments of limestones with Devonian corals (Linnemann, 2004). It is also based on the correlation with lithological profiles of the autochthonous Thuringian and allochthonous Bavarian facies of the Saxothuringian Basin where metabasalts are underlain by paleontologically dated limestones, which in some profiles pass into the early Carboniferous (Gattendorfia Kalk, Kohlenkalk; see Linnemann et al., 2008b, for details). The Lower to Middle Mississippian age of the basaltic lavas is also postdated by the positions of keratophyre tuffs within the Mississippian coal-bearing limestones, which yielded U–Pb zircon age of 347 ± 4 Ma (Gehmlich et al., 2001). The entire allochthonous complex is then overlain by discordant late Visean flysch of Striegis Formation and early Variscan molasse with layers of the late Viséan tuffs yielding an age of 330 ± 4 Ma (Linnemann et al., 2008a). This early Variscan molasse (Hainichen Subgroup) postdates the formation of the rift-related pillow lavas in this part of the Saxothuringian Basin (Gaitzsch et al., 2010; Gehmlich et al., 2003). Some of the lithological units exposed in the Frankenberg allochthon continue through the Nossen Wilsdruff Schiefergebirge into the Elbtalschiefergebirge, where they are tectonically reduced and imbricated on the Elbe Shear Zone, which experienced ductile deformation between ca. 342 and 327 Ma (Hofmann et al., 2009) and was later reactivated multiple times in the brittle regime.

The metabasites of the Elbtalschiefergebirge, intercepted by drill hole VRT_D_1 (**Fig. 3**), are exposed in the tectonically uppermost slice underlying the Weesenstein Fault, part of the West Lusatian Fault zone (**Fig. 2**). Both the metasediments with partially preserved magmatic structures and strongly foliated amygdaloidal lavas are present. They alternate with marbles at cm to several ten centimeters intervals between 148.8 m and 165.7 m and thus probably represent basaltic tuffs (**Fig. 3**). The inferred Middle to Late Devonian age results from correlation with similar rocks exposed in quarries near Křižany in the Ještěd Mts. area, where their Devonian age is supported by paleontological findings (Chlupáč, 1993), indicating a Middle to Late Devonian age of the limestones. Basic and acidic volcanic rocks occur in this sequence (Jítrava Group according to Chaloupský, 1989). Porphyroid intercalated with limestone on the SE of Vápenný hill (**Fig. 2d**) yielded a Middle Devonian age of 386.8 ± 1.7 Ma (**Fig. 8**). However, it is possible that some metadolerites with less steep REE profiles, akin to transitional MORB basalts, as well as lavas interleaving flysch sediments W of Kryštofovo Údolí may also be early Carboniferous in age. In the tectonically lower slice of the Elbtalschiefergebirge, interpreted by facies evolution as a part of the autochthonous Thuringian Facies, metarhyolites alternating with mafic lavas and metasediments with Famennian ages of 369 ± 8 Ma have been found (Königshof and Linnemann, 2008). This strongly supports the presence of Middle to Upper Devonian volcanism in both Thuringian and Bavarian facies of the Devonian Elbtalschiefergebirge.

Amygdaloidal lavas are exposed in the Jítrava Group (Middle Devonian to early Carboniferous) in the northern part of the Ještěd Mts. (**Fig. 2d**). Metadolerite JG-9 appears to represent a feeder dyke directly in the amygdaloidal lava complex, whereas sample ZB-443 intruded fine-grained laminated phyllitic shales with layers of fine-grained Late Devonian to early Carboniferous graywackes of the Jítrava Group. The age of the metadolerite dykes (JG-260), which penetrate older Ordovician orthogneiss, cannot be considered without the uncertainty because alkaline metabasites also are common in autochthonous units of the Krkonoše Crystalline Unit, where they crop out together with tholeiitic lavas in the Železný Brod and Rýchory volcanic complexes, which are Cambro-Ordovician in age (Klomínský et al., 2006, Kozdroj et al., 2005, Patočka et al., 2000).

The brecciated pillow and amygdaloidal basalts occur in association with alkali rhyolites to trachytes, which alternate with crystalline limestones (Kozdroj et al., 2005) at the Malý Vápenný Hill, NW of Křižany. The age of the metarhyolite, intercalated within the limestone body in a quarry s. of Křižany, corresponds to the Eifelian–Givetian boundary (U–Pb zircon age of 386.8 ± 1.7 Ma; this study). Amygdaloidal lavas, however, occur in the N flank of the anticline in which the transition from Devonian to Carboniferous is paleontologically documented on the basis of goniatite and trilobite faunas (Chlupáč, 1964, 1993). Thus, some lava flows occurring within flysch of the Jítrava Group are up to early Carboniferous in age, evidenced by their occurrences within the weakly metamorphosed and strongly ductile-deformed flysch sequence with numerous tens of centimeters thick layers of intraformational and polymictic fine-grained conglomerates that contain abundant mounds of silicified black shales, lydites, acidic volcanic rocks and limestones derived from underlying rock complexes.

Collectively, the stratigraphy and new geochronological data from this study provide conclusive evidence for widespread basaltic volcanism along the N Gondwana margin starting with Mid Devonian bimodal metabasite–rhyolite association and continuing up to Early Carboniferous with the peak of dominantly basaltic members around the Devonian to early Carboniferous boundary (**ESM 7**).

5.2 The spatial extent of rift-related volcanism within the Saxothuringian Zone and its tectonic relevance

Within the Saxothuringian Zone, intraplate rift-related volcanic rocks are widespread in three areas:

(i) The Vesser River area, where Cambro–Ordovician ~ 505 Ma bimodal volcanism is interpreted as a product of either a failed rift (Bankwitz, 1998) or intra-arc basin magmatism (Linnemann et al., 2010), dividing the Saxothuringian microplate into two sub-blocks, northern Franconia and southeastern Thuringia (Franke et al., 2017).

(ii) The SE edge of Saxothuringia, following the discontinuously observed Saxothuringian or Teplá suture (**Fig. 1**), records a greater extent of Cambro-Ordovician bimodal extension-related volcanism. Cambrian–Ordovician volcanic rocks are widespread in the Frankenwald, and Vogtland, in the western, northern and, to a lesser extent, eastern surroundings of the Münchberg klippe. Cambro–Ordovician volcanic sequences are present in both the autochthonous Thuringian facies as well as the allochthonous Bavarian facies (Bahlburg et al., 2010; Höhn et al., 2018; Koglin et al., 2018; Martin et al., 2003). Basic alkali basaltic sills and thin layers of contact-metamorphosed basic tuffs occur in the Frauenbach Group between Jáchymov and Pernink, and near Potůčky. A similar, relatively thick sill intruded into the Ordovician rocks of the Phycodes Group in the Smrčiny/Fichtelgebirge Mts. east of the Münchberg Nappe (Lucassen et al., 2025). Occurrences of Silurian alkaline volcanic rocks west of the Münchberg Nappe are rare. Minor bodies of rhyolites and their pyroclastic counterparts of late Cambrian to Early Ordovician age (486 ± 4 Ma and 479 ± 5 Ma) are present in the Schwarzburg anticline (Linnemann et al., 2010) and in the Frauenbach Group at the transition from the Smrčiny/Fichtelgebirge–Krušné hory/Erzgebirge Mts. anticline to the Vogtland syncline (Gehmlich, 2003).

(iii) The Lugian (Sudetic) part of the Saxothuringia also hosts bimodal Cambrian–Ordovician volcanic rocks (508 Ma to ~480 Ma) of E-MORB, N-MORB and alkali intraplate basalt types, associated with both juvenile metarhyolites with positive ε_{Ndi} values and crustal melts with negative ε_{Ndi} signature (Floyd et al., 2000, Furnes et al., 1994; Jastrzebski, M., et al., 2026; Kachlík, unpubl.; Mlynarska et al., 2023; Patočka and Dostal, 1997; Dostal et al., 2001). Basaltic volcanic rocks are volumetrically important, especially in the Železný Brod Volcanic Complex, Rýchory Mts. and Kaczawa Mts. (Bendl and Patočka, 1995; Furnes et al., 1994; Kozdroj et al., 2005; Patočka et al., 2000; Patočka and Pin, 2005). These units mostly correspond to the paraautochthonous Thuringian facies. Both juvenile and crustal felsic melts are subordinate. Isolated occurrences of the late Cambrian rhyolites (501 ± 3 Ma) are also described from the Kłodzko area (Mazur et al., 2015).

Cambrian felsic volcanic rocks overlap in time with the very widespread Cambrian–Ordovician orthogneisses, which are known from the Schwarzburg anticline as well as from allochthonous units (Münchberg Massif, Frankenberg), Elbtalschiefergebirge, Smrčiny/Fichtelgebirge, Krušné hory/Erzgebirge, Jizerské hory, Krkonoše and Orlické hory, the Kłodzko Crystalline Complex and the Góry Sowie Crystalline Complex. They are mainly represented by peraluminous S-types, which were formed by melting of the lower continental crust (Kröner et al., 1994; Mingram et al., 2004; Oberc-Dziedzic et al., 2009; Pin et al., 2007; Siebel et al., 1997). An exception is the Paczyn gneiss (515–495 Ma) in the Rýchory Mts., which has a highly enriched Sr–Nd isotopic signature and is interpreted as a product of melting above the subduction zone separating the Teplá–Barrandian plate from the Saxothuringian microplate in the intra-oceanic island arc (Młynarska et al., 2023, Oliver et al., 1993).

Devonian bimodal volcanic rocks are predominantly limited to the SE edge of Saxothuringian unit, with the largest distribution in the autochthonous Thuringian facies around the Münchberg klippe, but they also are present in basal slices of the allochthonous Bavarian facies occurring near the base of the Münchberg klippe, and its equivalents (i.e., Wildenfels, Frankenberg, Elbetalschifergebirge and Ještěd Mts.). The presence of this volcanosedimentary sequence cannot be excluded in the same tectonic position below the Mariánské Lázně Complex and Zone Erbendorf–Vohenstrauss, where alkaline lavas occur within black shales with lydites (Wetzeldorf and Kladská Unit). These alkaline lavas were correlated with Cambro–Ordovician or Silurian strata (Wetzeldorf unit; Kachlík, 1993; Lapp, 1995), but according to the presence of Devonian clastic zircons, they might be Devonian in age.

Pillow lavas in the Seifersdorf quarry crop out near the base of the allochthonous Frankenberg klippe. Their bedrock contains dark graphitic silicified phyllitic schists, which in the Saxothuringian basin range from early to Lower to Middle Devonian. Therefore, lava extrusion most likely occurred during the Frasnian, at a time when Devonian basic volcanism in the Thuringian part of the Saxothuringian unit reached its climax (Gandl, 1989). Felsic tuffs were also documented in the tectonically higher part of the same slice of the Frankenberg allochthonous klippe. The Pb–Pb zircon ages of 357 ± 2 Ma and 351 ± 2 Ma indicate their Famennian to Turnaisian affiliation (Gehmlich, 2003). Slightly younger metarhyolites (369 ± 5 Ma in comparison with the Ještěd Mts. area) also occur within imbricated slices of the Elbe Shear Zone (**Fig. 2c**). This slice including Devonian metabasalts is assumed to be derived from paraautochthonous Thuringian facies. Similarly old rhyolites (375 ± 4 Ma) were also reported in the Thuringian facies of the Berga anticline (Gehmlich, 1998).

Basic lavas, metatuffs and metadolerites studied in the borehole VRT_D_1 which alternate with limestones and black phyllitic shales, belong tectonically to the highest tectonic slice of the Elbe Shear Zone (**Fig. 2**), which is lithologically parallel with the Upper Devonian of the Bavarian Facies (Königshof and Linnemann, 2008). Metadolerites, forming sills or dykes may be up to early Carboniferous in age, particularly sample VRT_D_1/81 showing E-MORB affinity. Similar limestones alternating with mafic tuffs, porphyroid and mafic lavas, as described in the borehole VRT_D_1 belonging to the Elbtalschiefergebirge, also crop out in the Jítrava Group on Ještěd Mts. in the NW surrounding of Křižany (**Fig. 2d**). The rocks of the Jítrava Group are newly interpreted as an allochthonous unit of the Bavarian facies due to facies similarities described above and tectonic position above the underlying paraautochthonous Paleozoic units in the E and Central part of the Ještěd Unit (Kachlík and Kozdroj, 2001), which include typical facies types such as Silurian Ockerkalk limestone (Chlupáč 1993). Devonian age was also given for alkaline metagabbro near Těpeře NW of the Železný Brod Volcanic Complex and dominantly alkaline dykes of metadolerites and microgabbros in the Jizera orthogneisses in the NW vicinity of Jelenia Góra (Nowak et al., 2011). This indicates a notably larger extent of Devonian alkaline volcanism related to the extension in the Krkonoše–Jizera region during the early to middle Carboniferous with the peak in the Frasnian–Famennian.

5.3 Compositional correlation within the Saxothuringian Zone

Differing tectonometamorphic histories of the correlated units result in differences in the observed mineral assemblages of the studied metabasalts. Despite significant recrystallization, the main rock-forming minerals or their relics survived and could be analyzed. The notably homogenous composition of clinopyroxene (**Fig. 5a,b**) indicates very similar composition of parental magmas, with the exception of sample VRT_D_1/81 where bulk-rock as well mineral chemistry point to distinct petrogenesis. Alkaline tendency of the parental magmas is evident from elevated Ti contents of clinopyroxene (again except the outlier sample VRT_D_1/81), where samples from Frankenberg deviate from other units (**Fig. 5c**). This departure in Mg–Ti compositional systematics does not appear to reflect a different source, but rather the increasing compatibility of Ti in the clinopyroxene lattice with decreasing pressure (Tracy and Robinson, 1977); this observation agrees with pillow lava character of Frankenberg samples. Eruptive character and super-cooling of submarine lavas also resulted in the absence of feldspar crystals; glass chloritized later formed in these lavas instead (**Fig. 4a**).

Newly-determined chemical compositions overlap with published data for Devonian dykes in the Jizera Mts. (Nowak et al., 2011), Devonian basalts of the Münchberg block (Höhn et al., 2018) and Silurian basalts of the Prague Basin (Tasáryová et al., 2018) in the TAS (**Fig. 6a**) and Nb/Y vs. Zr/Ti (**Fig. 6b**) plots. Ordovician and Silurian volcanic rocks of the Münchberg block are distinguished by higher alkalinity and a clearly defined differentiation trend extending from picrobasalts towards trachyandesites (**Fig. 6a**). All studied Devonian rocks in the Saxothuringian together with Silurian basalts of the Prague Basin plot within the alkali basalt field with transition to subalkaline basalts and displaying Nb/Y <1.7, whereas older (Ordovician–Silurian) volcanic rocks of the Münchberg block display a well-constrained alkaline (Nb/Y >1.7) differentiation trend extending to tephriphonolites. The notable deviation of Frankenberg lavas towards less alkaline character (**Fig. 6b**) may underscore a higher degree of melting resulting in a more tholeiitic trend. Such a hypothesis is also supported by the excursion of Frankenberg samples towards MORB compositions in the La/Yb vs. Nb/La and Th–Hf/3–Nb/16 discrimination plots (**Fig. 6c,d**). Greater degrees of partial melting in Frankenberg samples compared with the other two suites from this study are further indicated by less steep REE patterns (**Fig. 7a**) and depletions in Nb, Ta, and Sr (**Fig. 7b,c**).

A compilation of available Nd isotopic data for pre-Variscan Paleozoic mantle-derived samples distributed throughout the Bohemian Massif is given in **Fig.9a**. Broadly speaking, most samples are variably depleted, with positive ε_{Nd} for their respective ages, and span most of the range between Bulk Silicate Earth (BSE) and the band representing a 2σ range of the observed depleted MORB-source mantle (Workman and Hart, 2005). The Frankenberg, Elbtalschiefergebirge, and Ještěd Mts. samples, taken as a group, are highly similar to the Münchberg sills or dykes (Lucassen et al., 2025) that are closest both in terms of geography and age. They are also comparable to the older Prague Basin volcanic rocks (Dostal et al., 2019; Tasáryová et al., 2018) and metavolcanics rocks of the Kaczawa Mts. to the east (Furnes et al, 1994). Besides, eclogites and amphibolites of the metaophiolite Mariánské Lázně Complex (Beard et al., 1995) as well as Ślęża ophiolites also appear to be comparable to samples from this study. Within the suites that comprise this study, the Frankenberg samples form a tight cluster, having the most radiogenic (MORB-like) Nd isotopic signatures, whereas the Elbtalschiefergebirge and Ještěd Mts. samples scatter in mutually overlapping ranges straddling the E-MORB portion of the DMM field and grading toward less radiogenic Nd isotopic compositions. This is consistent with trace element data that also indicate a transition from intraplate to MORB-like character. Moreover, Pb isotope compositions for both Ordovician (Lucassen et al., 2025) and Devonian (this study) rift-related volcanic rocks broadly overlap (**Fig. 9b**). They are slightly oblique to mantle-like trend and increasing $^{207}Pb/^{204}Pb$ ratio reflects, apart from variable sources, also variable melting degree, isotopic fractionation and crust assimilation, which reaches the greatest extent in Ordovician lavas from the allochthonous and autochthonous units cropping out west of the Münchberg Massif.

Broadly similar compositions of the three correlated suites encompassing the transition from OIB (within-plate or continental rift) to MORB-like composition are in accord with early stages of oceanic rift development probably in the area of the present Saxothuringian suture further to SE, as is also reflected in chemistry of mildly alkaline metabasalts of the Kladská Unit (Crowley et al., 2003) and alkaline to tholeiitic metabasalts in the Prasinite–Phyllite unit of Münchberg klippe (Höhn et al., 2018). A tendency of the Frankenberg samples toward more MORB-like composition including less steep REE patterns indicates that Frankenberg Devonian volcanic rocks were probably emplaced closer to the NW flank of the opening Saxothuringian Ocean tract. This is consistent with more developed rifting in the western part of the investigated zone and progressive west-to-east rift propagation. Another possibility is a variable rate of along strike propagation of the rift branches as is observed in the Cenozoic East African Rift, with progressive propagation of the rifting and associated changes in composition of erupted lavas from OIB-like to MORB-like chemistry (Biggs et al., 2021). We therefore posit that the evolution and spatial distribution of eruptive products from Paleozoic rifting documented here has common aspects to those observed in a modern example of an analogous process.

6. Geotectonic evolution of the Saxothuringian Zone in relation to evolution of the northern Gondwanan margin

6.1 Plate tectonic reconstructions and models of Central European Variscides

Plate tectonic reconstruction of Variscan Western and Central Europe has long been discussed and there are a number of models that explain both the Cambro–Ordovician breakup of the northern edge of Gondwana and its causes – back-arc spreading, extension linked to far field forces connected with subduction of the Laurentian part of Iapetus Ocean or Tornquist Sea on the opposite SW passive margin of the Rheic Ocean (in relative geographic coordinates), plume-related extension, or basaltic underplating (e.g., Crowley et al., 2000; Linnemann et al., 2008a; Martínez Catalán et al., 2020). This then also leads to the yet unconstrained number of oceanic tracts and sutures that might have existed and the kinematics of their closure.

Most models agree on the existence of the Rheic Ocean, which formed after the Cambrian rifting of Avalonia and related terranes (Brunovistulicum, Malopolska, Moesia, Istanbul-Zonguldac) derived from the Amazonian part of Peri-Gondwana (Franke, 2024; Cox and Torsvik, 2002; Linnemann et al. 2007; Murphy et al. 2006; van Staal et al. 1998; von Raumer and Stamfli, 2008; Winchester et al., 2002). At the same time, these models differ in the timing of its closure. While Zeh and Gerdes (2010) brought arguments for Silurian to early Devonian closure of the Rheic Ocean under the margin of Avalonia–Baltica (so-called Ballonia), zircon ages indicate that closure of the Rheic Ocean by bilateral subduction continued until the Lower Carboniferous. According to this model, the Middle Devonian to early Carboniferous rift volcanism on the southeastern margin of Avalonia is associated with the back extension behind the oceanic arc on the NW flank of the Rheic Ocean (Nesbor, 2025). Alternative models connect closure of the Rheic Ocean by subduction under an oceanic arc and its accretion to Avalonia in the Silurian and reopening of the Rhenohercynian Ocean during the Devonian and Carboniferous (Franke 1989a,b; Franke and Zelazniewicz, 2023). Similar to the model of Nesbor (2025), these models assume bilateral closure of the subsequent Rhenohercynian Ocean under both the continental margins of Avalonia in the NW and Saxothuringia in the SE (Franke, 2024). The competing group of models is represented by those explaining the presence of MORB-type rocks and ultramafic mantle lithologies by extension of deeper parts of the Gondwana shelf (passive margin) during Cambro–Ordovician or younger extensional periods. In these models, Saxothuringian, Bohemian and Moldanubian ribbon continents were not separated from the Gondwanan mainland and, therefore, they lack any lines of reasoning for the existence of any of the above-mentioned oceans (Linnemann et al., 2004; Žák and Sláma, 2018).

In most of the discussed models, a broad consensus exists about the existence of the Saxothuringian Ocean between the Saxothuringian and Teplá–Barrandian units, which represents a southern tract of the Rheic Ocean. Its existence is indicated by SE-directed under-thrusting of the Mariánské Lázně ophiolite Complex under the Teplá–Barrandian Unit. Relic ophiolitic fragments, which provide unequivocal evidence of subduction of the Saxothuringian passive margin even on order of several tens km, occur in the allochthonous complexes such as Zone Erbendorf–Vohenstrauss, Münchberg Massif and Frankenberg klippe, all of which contain high-pressure rocks with MORB-like chemistry (e.g., Beard et al., 1995; Collet et al., 2018; Crowley et al., 2002; Franke, 1989a,b; Kachlík,1993). The persisting problem central to these models is the protolith age and time of eclogite-facies metamorphism of eclogites and garnet amphibolites, which may be Cadomian (Neoproterozoic to Lower Cambrian; e.g., Timmermann et al., 2004), because they are intruded in the Mariánské Lázně

Complex by Cambro–Ordovician Ti-rich intraplate-type metagabbros (Štědrá et. al.; 2002) which are devoid of eclogite-facies metamorphism. Another possibility is an Ediacaran to Cambrian protolith age of eclogites and Mid-Devonian eclogite-facies metamorphism (Collet et al., 2018, 2022 and references therein). The Devonian age of the Prasinite-Phyllite Group sediments, which contain lenses of serpentinites as well as alkali and tholeiitic metabasalts (Koglin et al., 2018), bordering the SE edge of the Münchberg Block, however, proves that there may also be Devonian ophiolites (e.g., Deiller et al., 2021). According to Deiller et al. (2021), high-pressure rocks of the Mariánské Lázně Complex and the upper plate of the Teplá–Barrandian Unit are penetrated by arc-related magmas such as gabbros and trondhjemites which may be connected with Devonian southeastward subduction of the Saxothuringian Ocean. Devonian (~ 400 Ma) ophiolites surrounding the Sowie Gory Mts. allochthon, often interpreted as continuation of the Teplá Suture (Franke et al., 2017 and references therein), should be derived from the Rheic/Rhenohercynian Suture dividing Brunovistulian and Lugodanubian domains (Faryad and Kachlík, 2013).

The third, southernmost branch of the assumed Rheic Ocean may be the Moldanubian Ocean between the Teplá–Barrandian Unit and the Moldanubicum s.s. The (U)HP Moldanubian rocks (garnet peridotites, eclogites) enclosed in granulites are interpreted either as exhumed blocks in the subduction channel during Late Devonian subduction and early Carboniferous collision of the Teplá–Barrandian Unit and Moldanubicum (Perraki and Faryad, 2014; Medaris et al., 2006) or as diapirs extruded from the subducted Saxothuringian lower crust (Schulmann et al., 2008)

6.2 Geotectonic significance of Ediacaran to early Carboniferous volcanism in Saxothuringia and Teplá–Barrandian

The final phases of the Cadomian orogeny associated with Cadomian calc-alkaline magmatism and volcanism end roughly at the Proterozoic/Cambrian boundary with intrusions of the youngest Cadomian plutonic rocks in the Lusatian massif at ~540 Ma (Żelaźniewicz et al., 2004). Calc-alkaline magmatism probably associated with Cadomian crustal melting of thickened crust continued up until the lower to middle Cambrian in the Teplá–Barrandian Unit (515–505 Ma; Dörr et al., 1998). Early to middle Cambrian extensional grabens and pull-apart basins unconformably overlain the Cadomian accretionary wedge, whose accretion waned out at ~527 Ma (Hajná et al., 2018) and was postdated by mantle-derived gabbroic massifs (Syahputra et al., 2023). In the both above-mentioned areas and also in the Moldanubian, late Cambrian to early Ordovician magmatism is widespread and volumetrically important (Drost et al., 2008; Oberc-Dziedzic et al., 2010; Siebel et al., 1997; Žák et al., 2023b; Patočka et al., 2000 and references therein).

In the Saxothuringian, bimodal volcanic rocks occur in the Frankenwald area from ca. 505 Ma according to U–Pb zircon ages and Thuringian Forest (**Fig. 10a**). Most of the basaltic members, differentiated up to trachybasalts in both the Bavarian and Thuringian facies, are part of thick Ordovician sequences, although geochronological data fall on the Cambrian–Ordovician boundary (486–480 Ma; Höhn et al., 2018). The metadolerite sills in the Frauenbach and Phycodes Groups are probably also Ordovician (Lucassen et al., 2025), but may be even younger. Late Cambrian to early Ordovician bimodal rift-related magmatism is volumetrically important also in the Krkonoše–Jizera Unit, Kaczawa Mts., where alkaline OIB-type magmas occur together with mantle-derived tholeiitic basalts (Patočka et al., 2000; Dostal et al., 2001; Furnes et al., 1994). The large thickness of Tremadocian strata in the Saxothuringian Basin and the presence of bimodal volcanic rocks, including both alkaline intraplate basalts to trachybasalts, rhyolites, alkali rhyolites, and T-MORB basalts, indicate the interaction of Ti-rich magmas derived from a deep mantle source, where in most cases garnet was in the residue, with shallower T-MORB or E-MORB-type sources probably originating from the subcontinental mantle. This process was repeated in the Silurian in both units, Saxothuringian and Prague Basin (Barrandian). However, in the Saxothuringian Unit, the presence of paleontologically documented Silurian volcanic rocks is rare.

Greater volumes of tholeiitic basalts in the Kaczawa Mts., Krkonoše–Jizera Crystalline unit, and the presence of juvenile subduction-related ~515 to 495 Ma orthogneisses, gabbros and metabasalts (Młynarska et al., 2023) and felsic rocks in the Železný Brod Volcanic Complex in South Krkonoše provide cumulative evidence that rift branches propagated to the NE (Patočka et al, 2000), or this unit originated in close relation to intraoceanic arc/backarc environment (Mlynarska et al., 2023). Pulse of juvenile magmatism may thus postpone slab pull after the end of Cadomian subduction.

In the Teplá–Barrandian Unit, volumetrically important Furongian subaerial calc-alkaline volcanic suites of basaltic to rhyolitic lavas and volcanoclastic rocks (Drost et al., 2004; Kachlík and Patočka, 1998; Patočka et al., 1992) overlie paleontologically documented middle Cambrian sequences. They have been interpreted either as volcanic arc rocks associated with Cadomian processes (Patočka et al., 1992) or as products associated with the formation of Cambrian asymmetric grabens (furrows) that arose in the extensional or transtensional regime (Drost, 2008; Drost et al., 2004; Žák et al., 2023). However, intercalated acidic tuffs as well as rhyolite dykes are demonstrably represented in the Ordovician, whereby the age of the former is connected with the underlying volcanic complexes (Žák et al., 2013), but the age of the latter cutting the Ordovican sediments remains unconstrained.

An abrupt change from calc-alkaline subaerial to submarine basaltic volcanism of intraplate OIB- to T-MORB-type began slightly later in the Prague Basin (Barrandian) than in the Saxothuringian Basin during the Floian with peak in the Darriwilian to Sandbian (**Fig. 10a**), continued with late Ordovician break to the Silurian (Llandovery and Ludlow;

Tasáryová et al., 2018) and terminated during the early Devonian (Fiala, 1970). In addition to basaltic members, olivine-rich meimechite sills (formerly known as picrites) occur within Silurian black shales (Fiala, 1970, Tasáryová et al., 2018), which either are ultramafic cumulates of basaltic magmas or represent melts formed from metasomatized garnet peridotites, which reacted with the depleted subcontinental lithospheric mantle during diapiric emplacement of magma. Both Silurian and Devonian basalts assimilated crustal material during the reaction with hot Ca–Sr–Ba-rich fluids on the seafloor or with water originating from the surrounding sediments (Patočka et al., 1992, Tasáryová et al., 2018).

In the Saxothuringian Basin, the third pulse of alkaline magmatism associated with transition to T-MORB with a small proportion of alkali rhyolites and rhyolites occurred during the Middle Devonian to early Carboniferous **(Fig. 10b**). On the contrary, this pulse is missing in the Barrandian area, where Variscan deformation started earlier in comparison with the Saxothuringian. Bimodal rhyolite–basalt association mainly was present in the Middle Devonian whereas alkaline basaltic magmas subsequently dominated. In the early Carboniferous, basaltic volcanism changed to tholeiitic chemistry. This volcanism was mostly interpreted as a product of arc extension in the area of the SE-dipping Rheic subduction zone (Kachlík and Patočka, 2001). However, volcanism of the same chemistry and stratigraphic extent also occurs in the Rhenohercynian region at the edge of the rifted part of Avalonia (**Fig. 10b**). Southward transition into tholeiitic members is observed in Giessenian nappes thrust over the passive margin of Avalonia (Franke, 2007; Nesbor, 2025; Salamon and Königshof, 2010). This type of volcanism, which is also associated with Devonian oolithic iron ores of the Lahn-Dill type, is also abundant in the Jeseníky Mts. and the Šternberk–Horní Benešov Volcanic belt **(Fig. 10b)**, exhumed from below Variscan flysch along E inclined back-thrust zone. The repetition of rift-related volcanism in similar stratigraphic intervals, over a large area and its shift towards the periphery strongly support long-term hot spot activity, which led to disintegration of the Gondwana margin in the Ordovician (Casas et al., 2024; Crowley et al., 2000; Murphy et al., 2024) and later reopened supply channels for intraplate magmatism, especially in the Rhenohercynian and Saxothuringian Basins during the Middle-Devonian to early Carboniferous (Franke and Żelaźniewicz, 2023). Plume-related rift fragmentation in a backarc region on northern side of the Rheic Ocean is observed in Avalonia and Brunovistulia as well as in the southern flank of the Rheic (Saxothuringia, southern Vosges) if double-sided subduction of the Rheic Ocean is considered.

In the case of the Rhenohercynian Ocean, this led to its reopening, as it affected not only the area at the Avalonian/Brunovistulian and Saxothuringian northwestern and northern boundary, but also its southeastern parts closer to the vicinity of the Teplá Suture. Given the presence of alkaline OIB-type and tholeiitic volcanism in the area of the present-day Eastern Alps (Guan et al., 2021; Neubauer et al., 2022) and Devonian ophiolites in Balkan, it cannot be ruled out that the plume-initiated extension and rifting may be connected with NW-ward subduction of the Moldanubian (Central European) Ocean between Armorican fragments and Paleo-Adria or Balkan–Carpathian Ocean, subsequent opening of the Paleotethys Ocean between Variscan Europe and northern Gondwana margin, and separation of Galatian terranes (Neubauer et al., 2022).

7. Conclusions

This study revisited the occurrences of metabasaltic rocks within the Saxothuringian Zone of the Bohemian Massif. The synthesis of the existing literature data and new data collected here allowed us to reconstruct the paleotectonic history and rift-related volcanism along the northern Gondwana edge, associated with the formation of several Rheic/Rhenohercynian and Saxothurignian Ocean tracts. From a thorough review of the available data, it is evident that the Saxothuringian region underwent three stages of extension during the Paleozoic, probably associated with long-term plume activity along the northern edge of Gondwana, which caused its gradual fragmentation associated with the formation of the Rheic, Saxothuringian and Moldanubian Oceans and ending with the opening of the late Paleozoic Paleotethys Ocean.

(1) The initial rifting falls in the period from the end of the Cambrian to the beginning of the Ordovician (ca. 505–470 Ma). The heat brought into the crust by the activity of a temporally persistent plume caused gradual thinning of the crust and the intrusion of mantle-derived OIB-like magmas, which at the SE edges of the Saxothuringian region in the Krkonoše and Kaczawa Mts. accompanied tholeiitic basalts, marking the transition from intracontinental rift to oceanic stage.

(2) Strongly alkaline OIB-type and highly fractionated basalts in the vicinity of the Münchberg klippe represent the second phase in the Saxothuringian. On the contrary, Silurian to Lower Devonian basalts in the neighboring Teplá–Barrandian Unit tend toward a dominant presence of enriched tholeiitic magmas derived at shallow depths of the subcontinental depleted mantle.

(3) The re-appearance in the Saxothuringian Basin of volumetrically dominant bimodal volcanism, later changed toward basic OIB-type lavas, occurred from the Middle Devonian to the beginning of the early Carboniferous, followed by the appearance of minor volumes of tholeiitic enriched or transitional intraplate basalts.

This third phase overlaps temporally and geochemically with volcanism in the Rhenohercynian Basin, which is interpreted as the back-arc extension of the Avalon foreland of the Rheic Ocean subducted northward below Avalonia, while volcanism in the Saxothuringian Basin is probably connected with the southward subduction of the Rheic Ocean under the Saxothuringian microplate. The presence of Devonian to Lower Carboniferous eclogites on both sides of the Saxothuringian ribbon continent provides evidence for Devonian closure of Rheic/Rhenohercynian and Saxothuringian Oceans. The presence of Devonian rift-related associations in the Variscan basement of the Alps, Carpathians and the Balkans suggests that Devonian closure of all branches of Central European oceans caused shift of rifting again to Gondwana margin and caused opening of the Paleotethys Ocean.

Acknowledgements – This study was supported by the Czech Science Foundation project 23-07625S (TM) and by institutional support from Charles University trough the Cooperation Programme (Research Area GEOL) (VK). The authors are extremely indebted to Matt Horstwood (British Geological Survey, Nottingham, UK) for rescuing and editing geochronological data. We are grateful to Prof. Ch. R. Martínez Catalán and the anonymous reviewer for their critical remarks, and to Nelson Eby for swift editorial handling.

Declaration of interests

The authors declare that they have no known competing financial interests or personal relationships that could have appeared to influence the work reported in this paper.

References

Alexowsky, W.; Wolf, L.; Kurze, M.; Tröger, K.A., 1997. Geologische Karte Blatt 5049 Pirna – 3. Aufl.- Sächs. Landesamt f. Umwelt u. Geologie, Freiberg.

Anders, E., Grevesse, N., 1989. Abundances of the elements: Meteoritic and solar. Geochim. Cosmochim. Acta 53, 197–214.

Bahlburg, H., Vervoort, J.D., DuFrane, S.A., 2010. Plate tectonic significance of Middle Cambrian and Ordovician siliciclastic rocks of the Bavarian Facies, Armorican Terrane Assemblage, Germany U–Pb and Hf isotope evidence from detrital zircons. Gondwana Res. 17, 223–235.

Beard, B.L., Medaris, L.G., Johnson, C.M., Jelinek, E., Tonika, J., Riciputi, L.R., 1995. Geochronology and Geochemistry of Eclogites From the Marianske Lazne Complex, Czech-Republic - Implications For Variscan Orogenesis. Geol. Rundsch. 84, 552–567.

Becker, H., 1928. Das Zwischengebirge von Frankenberg in Sachsen. Abh. Sächs. Geol. Landesamt 8, 1–89.

Behr, H.J., Engel, W., Franke, W., 1980. Münchberger Gneissmasse und Bayerischer Wald (Excursion guide to the International conference on The Effect of Deformation on Rocks), Göttingen, April 9–12, 1980.

Bendl, J., Patočka, F., 1995. The ^{87} Rb ^{86} Sr isotope geochemistry of the metamorphosed bimodal volcanic association of the Rýchory Mts. Crystalline Complex, West Sudetes, Bohemian Massif. Geol. Sudet. 29, 3–18.

Berger, H. J., 2021. Geologische Übersichtskarte 1:200 000, CC 5542 Dresden. Bundesanstalt für Geowissenchaftern und Rohstoffe., Hannover.

Bialek, D., Kryza, R., Oberc-Dziedzic, T., Pin, C., 2014. Cambrian Zawidow granodiorites in the Cadomian Lusatian Massif (Central European Variscides): what do the SHRIMP zircon ages mean? J. Geosci. 59, 313–326.

Biggs, J., Ayele, A., Fischer, T.P., Fontijn, K., Hutchison, W., Kazimoto, E., Whaler, K., Wright, T.J., 2021. Volcanic activity and hazard in the East African Rift Zone. Nature Commun. 12, 6881.

Casas, J.M., Murphy, J.B., Díez Montes, A., Sánchez-García, T., de Poulpiquet, J., Álvaro, J.J., Guimerà, J., 2024. Does the Ollo de Sapo magmatic event support Furongian–Tremadocian mantle plume activity fringing NW Gondwana? Int. Geol. Rev. 66, 1956–1970.

Chaloupský, J., ed., 1989. Geologie Krkonoš a Jizerských hor. Ústř. Úst. geol., Praha, p. 288.

Chlupáč, I., 1964. Ein neuer Faunenfund im schwach metamorphisierten Paläozoikum von Ještědské pohoří (Jeschkengebirge, Nordböhmen) (in Czech, German summary). Čas. Mineral. Geol. 9, 27–35.

Chlupáč, I., 1993. Stratigraphic evaluation of some metamorphic units in the N part of the Bohemian Massif. N. Jb. Geol. Palaont. Abh. 188, 363–388.

Chlupáč, I., Hladil, J., 1992. New Devonian occurences in the Ještěd Mts. North Bohemia. Čas. Miner. geol. 37, 185–191.

Cocks, L., Torsvik, T., 2002. Earth geography from 500 to 400 million years ago: a faunal and palaeomagnetic review. J. Geol. Soc. 159, 631–644.

Collett, S., Schulmann, K., Deiller, P., Štípská, P., Peřestý, V., Ulrich, M., Jiang, Y., de Marien, L.d.H., Míková, J., 2022. Reconstruction of the mid-Devonian HP-HT metamorphic event in the Bohemian Massif (European Variscan belt). Geosci. Front. 13, 101374.

Collett, S., Štípská, P., Schulmann, K., Peřestý, V., Soldner, J., Anczkiewicz, R., Lexa, O., Kylander-Clark, A., 2018. Combined Lu-Hf and Sm-Nd geochronology of the Mariánské Lázně Complex: New constraints on the timing of eclogite-and granulite-facies metamorphism. Lithos 304, 74–94.

Crowley, Q.G., Floyd, P.A., Štědrá, V., Winchester, J., Kachlík, V., Holland, G., 2002. The Mariánské Lázně Complex, - (northwestern) Bohemian Massif: development and destruction of an Early Paleozoic saxothuringian seaway. J. Geol. Soc. London, Spec. Publ. 201, 157–177.

Crowley, Q.G., Floyd, P.A., Winchester, J.A., Franke, W., Holland, J.G., 2000. Early Palaeozoic rift-related magmatism in Variscan Europe: fragmentation of the Armorican Terrane Assemblage. Terra Nova 12, 171–180.

Deiller, P., Štípská, P., Ulrich, M., Schulmann, K., Collett, S., Peřestý, V., Hacker, B., Kylander-Clark, A., Whitechurch, H., Lexa, O., 2021. Eclogite subduction wedge intruded by arc-type magma: the earliest record of Variscan arc in the Bohemian Massif. Gondwana Res. 99, 220–246.

Dörr, W., Fiala, J., Vejnar, Z., Zulauf, G., 1998. U-Pb zircon ages and structural development of metagranitoids of the Teplá crystalline complex - evidence for pervasive Cambrian plutonism within the Bohemian Massif (Czech Republic). Geol. Rundsch. 87, 135–149.

Dörr, W., Finger, F., Linnemann, U., Zulauf, G., 2004. The Avalonian-Cadomian Belt and related peri-Gondwanan terranes. Int. J. Earth Sci. 93, 657–658.

Dostal, J., Murphy, J.B., Shellnutt, J.G., 2019. Secular isotopic variation in lithospheric mantle through the Variscan orogen: Neoproterozoic to Cenozoic magmatism in continental Europe. Geology 47, 637–640.

Dostal, J., Patočka, F., Pin, C., 2001. Middle/Late Cambrian intracontinental rifting in the central West Sudetes, NE Bohemian massif (Czech Republic); geochemistry and petrogenesis of the bimodal metavolcanic rocks. Geol. J. 36, 1–17.

Drost, K., Linnemann, U., McNaughton, N., Fatka, O., Kraft, P., Gehmlich, M., Tonk, C., Marek, J., 2004. New data on the Neoproterozoic - Cambrian geotectonic setting of the Tepla-Barrandian volcano-sedimentary successions: geochemistry, U-Pb zircon ages, and provenance (Bohemian Massif, Czech Republic). Int. J. Earth Sci. 93, 742–757.

Faryad, S.W., Kachlík, V., 2013. New evidence of blueschist facies rocks and their geotectonic implication for Variscan suture(s) in the Bohemian Massif. J Metam. Geol. 31, 63–82.

Fiala, F., 1970. Silurské a devonské diabasy Barrandienu. Sbor. geol. Věd, řada G 17, 7–89.

Floyd, P.A., Leveridge, B.E., Franke, W., Shail, R., Dorr, W., 1990. Provenance and Depositional Environment of Rhenohercynian Synorogenic Greywackes from the Giessen-Nappe, Germany. Geol. Rundsch. 79, 611–626.

Floyd, P.A., Winchester, J., Seston, R., Kryza, R., Crowley, Q.G., 2000. Review of geochemical variation in Lower Palaeozoic metabasites from the NE Bohemian Massif: intracontinental rifting and plume-ridge interaction, in: Franke, W., Haak, V., Oncken, O., Tanner, D. (Eds.), Orogenic processes: Quantification and modelling in the Variscan Belt. Geol. Soc. London, Spec. Publ., London, pp. 155–175.

Franke, W., 1989a. Tectonostratigraphic units in the Variscan belt of central Europe. Geol. Soc. Amer. Spec. Pap. 230, 67–89.

Franke, W., 1989b. Variscan Plate-Tectonics in Central-Europe - Current Ideas and Open Questions. Tectonophys. 169, 221–228.

Franke, W., 1992. Phanerozoic structures and events in central Europe, In: Blundell, D., Freeman, K., Mueller, A. (Eds.), A continent Revealed - The European Geotraverse. Cambridge Univ. Press, pp. 164–179.

Franke, W., 2007. Rheno-Hercynian belt of central Europe: Review of recent findings and comparisons with south-west England. Geosci. South-West England 11, 263–272.

Franke, W., 2024. The Rheic riddle: ocean closed, but no orogen. Geol. Soc. London Spec. Publ. 542, 341–357.

Franke, W., Cocks, L.R.M., Torsvik, T.H., 2017. The Palaeozoic Variscan oceans revisited. Gondwana Res. 48, 257–284.

Franke, W., Żelaźniewicz, A., 2023. Variscan evolution of the Bohemian Massif (Central Europe): Fiction, facts and problems. Gondwana Res. 124, 351–377.

Franke, W., Zelazniewicz, A., Porebski, S.J., Wajsprych, B., 1993. The Saxothuringian zone in Germany and Poland: differences and common features. Geol. Rundsch. 82, 583–599.

Furnes, H., Kryza, R., Muszynski, A., Pin, C., Garmann, L.B., 1994. Geochemical evidence for progressive, rift-related early Paleozoic volcanism in the western Sudetes. J. Geol. Soc. 151, 91–109.

Gaitzsch, B., Egenhoff, S., Hesse, S., Ehling, B., Linnemann, U., Romer, R., 2010. Variscan early molasses in the Saxo-Thuringian. Pre-Mesozoic geology of Saxo-Thuringia, 311–322.

Galle, A., Chlupáč, I., 1976. Finds of corals in metamorphic Devonian of the Ještědské pohoří Mountains. Věst. Ústř. Úst. Geol 51, 123–127.

Gandl, J., 1989. Zum Aleter der Schwärzschifer und des hangenden Diabas-Vulkanismus im Devon des Frankewaldes (NE Bayern). Z. dt. geol. Ges. 140, 117–135.

García-Arias, M., Camera, M.M., Dahlquist, J., Gao, P., Couzinié, S., Díez-Montes, A., 2024. The tectonic significance of peri-Gondwanan Late Neoproterozoic-Early Palaeozoic felsic peraluminous magmatism. Earth-Sci. Rev. 254, 104803.

Gehmlich, M., Linneman, U., Tichomirová, M., Todt, W., Bombach, K., 1998. Geocheronologie und geochemische Signaturen devonischer Granitgerölle des Saxothuringikums und deren potentielle Liefergebiete des Saxothuringikum und deren potentielle Liefergebiete (Hirschberger Granit und Porphyroide von Neumühle/Greiz. Zt. Geol. Wiss. 26, 421–424

Gehmlich, M., 2003. Die Cadomiden und Variszíden des Saxothuringischen Terranes - Geochronologie magmatischer Ereignisse. Freiberger Forschungshefte 500, 1–129.

Gehmlich, M., Linnemann, U., Tichomirowa, M., Gaitzsch, B., Bombach, K., 2001. Geochronology of Late Devonian to Lower Carboniferous igneous rocks of Thuringian and Bavarian facies, Variscan crustal stacks and the early Variscan Molasse (Hainichen Basin) (Saxo-Thuringian Terrane). Zt. dt. Geol. Ges. 151, 337–363.

Guan, Q., Liu, Y., Neubauer, F., Li, S., Genser, J., Yuan, S., Chang, R., Huang, Q., Fang, Q., 2021. Opening of the West Paleo-Tethys Ocean: New insights from earliest Devonian meta-mafic rocks in the Saualpe crystalline basement, Eastern Alps. Gondwana Res. 97, 121–137.

Hajná, J., Žák, J., Dörr, W., Kachlík, V., Sláma, J., 2018. New constraints from detrital zircon ages on prolonged, multiphase transition from the Cadomian accretionary orogen to a passive margin of Gondwana. Precamb. Res. 317, 159–173.

Hofmann, M., Linnemann, U., Gerdes, A., Ullrich, B., Schauer, M., 2009. Timing of dextral strike-slip processes and basement exhumation in the Elbe Zone (Saxo-Thuringian Zone);

the final pulse of the Variscan Orogeny in the Bohemian Massif constrained by LA-SF-ICP-MS U-Pb zircon data. Geol. Soc. London Spec. Publ. 327, 197–214.

Höhn, S., Koglin, N., Klopf, L., Schüssler, U., Tragelehn, H., Frimmel, H.E., Zeh, A., Brätz, H., 2018. Geochronology, stratigraphy and geochemistry of Cambro-Ordovician, Silurian and Devonian volcanic rocks of the Saxothuringian Zone in NE Bavaria (Germany)—new constraints for Gondwana break up and ocean–island magmatism. Int. J. Earth Sci. 107, 359–377.

Hollocher, K., Robinson, P., Walsh, E., Roberts, D., 2012. Geochemistry of amphibolite-facies volcanics and gabbros of the Støren Nappe in extensions west and southwest of Trondheim, Western Gneiss Region, Norway: a key to correlations and paleotectonic settings. Amer. J. Sci. 312, 357–416.

Jastrzebski, M., Machowiak, K., Zelazniewicz, A., Sliwinski, M., Sláma, J., Fuenlabrada, J.M., Miková, J., Jazwa, A., 2026. Cambrian initiation of the Saxothuringian Ocean: New insights from the Kaczawa Complex, West Sudetes, Poland. Gondwana Res. 149, 212–228.

Kachlík, V., 1993. The evidence for Late Variscan nappe thrusting of the Mariánské Lázně Complex over the Saxothuringian (West Bohemia). J. Czech Geol. Soc. 38, 43–58.

Kachlík, V., 1994. The Kladská unit - petrological and structural evidence for Variscan thrusting of the Mariánské Lázně Complex over the Saxothuringian terrane (West Bohemia). KTB-Report 94, 3, 19–31.

Kachlík, V., Kozdroj, W., 2001. Ještěd Range Unit., In: Kozdroj, W., Krentz, O., Opletal, M. (Eds.), Comments on the Geological map Lauzitz - Jizera - Karkonozse (without Cenozoic sediments). Sächsisches Landesamt für Umwelt und Geologie/Bereich Boden und Geologie, Freiberg, Panstwowy Institut Geologiczny, Warzsawa. Český geologický ústav Praha, Warzsawa, pp. 27–31.

Kachlík, V., Kozdroj, W., 2001. Ještěd Range Unit., In: Kozdroj, W., Krentz, O., Opletal, M. (Eds.), Comments on the Geological map Lauzitz - Jizera - Karkonozse (without Cenozoic sediments). Sächsisches Landesamt für Umwelt und Geologie/Bereich Boden und Geologie, Freiberg, Panstwowy Institut Geologiczny, Warzsawa. Český geologický ústav Praha, Warzsawa, pp. 27–31.

Kachlík, V., Patočka, F., 1998. Cambrian/Ordovician intracontinental rifting and Devonian closure of the rifting generated basins in the Bohemian Massif realms. Acta Univ. Carol. Geol., 42, 433–441.

Kachlík, V., Patočka, F., 2001. Late Devonian to Early Carboniferous bimodal volcanic rocks of the Ještěd Range Unit: constraints on the development of the Variscan orogenic wedge. Geolines 13, 74–75.

Klomínský, J., Adamová, M., Burda, J., Jarchovský, T., Kachlík, V., Kořán, V., Kříbek, B., Manová, M., Nekovařík, Č., Šalanský, K., 2006. Vysvětlivky k základní geologické mapě České republiky 1: 25 000, 03-322 Jablonec nad Nisou. Česká geologická služba, Praha.

Koglin, N., Zeh, A., Franz, G., Schüssler, U., Glodny, J., Gerdes, A., Brätz, H., 2018. From Cadomian magmatic arc to Rheic ocean closure: the geochronological-geochemical record of nappe protoliths of the Münchberg Massif, NE Bavaria (Germany). Gondwana Res. 55, 135–152.

Königshof, P., Linnemann, U, 2008. The Rheno-Hercynian, Mid-German Crystalline and Saxo-Truringian Zones (Central European Variscides), Excursion Guide, 20 th. International Senckenberg-Conference and 2nd Geinitz-Conference: "From Gondwana and Lauriussia to Pangea: Dynamic of Oceans and Supercontinents", Final Meeting of GCPC 497 and IGCP 499. Senckenberg Forschunginstitut und Naturmuseum Frankfurt, Germany.

Kostitsyn, Y.A., 2007. Relationships between the chemical and isotopic (Sr, Nd, Hf, and Pb) heterogeneity of the mantle. Geochem. Int. 45, 1173–1196.

Kozdroj, W., Turniak, K., Tichomirová, M., Bombach, K., Kachlík, V., Ziolkovska-Kozdroj, M., 2005. New $^{207}Pb/^{206}Pb$ zircon ages from the East Krkonoše Metamorphic Complex, West Sudetes - Evidences of the Late Cambrian-Early Ordovician Magmatism. Geolines 19 (2005), 69–70.

Kraft, P., Linnemann, U., Mergl, M., Bruthansová, J., Laibl, L., Geyer, G., 2023. Ordovician of the Bohemian Massif, In: Harper, D.A.T., Lefebvre, B., Percival, I.G., Servais, T. (Eds.), A Global Synthesis of the Ordovician System: Part 1. Geol. Soc. London Spec. Publ. 532, 433.

Krmíčková, S., Krmíček, L., Romer, R.L., Ulrych, J., 2020. Lead isotope evolution of the Central European upper mantle: Constraints from the Bohemian Massif. Geosci. Front. 11, 925–942.

Kröner, A., Jaeckel, P., Opletal, M., 1994. Pb-Pb and U-Pb zircon ages for orthogneisses from Eastern Bohemia: Further evidence form a major Cambro-Ordovician magmatic event. J. Czech Geol. Soc. 39, 61.

Kroner, U., Hahn, T., Romer, R.L., Linnemann, U., 2007. The Variscan orogeny in the Saxo-Thuringian zone—heterogenous overprint of Cadomian/Paleozoic Peri-Gondwana crust. Geol. Soc. Amer. Spec. Pap. 423, 153–172.

Kroner, U., Romer, R.L., 2013. Two plates — Many subduction zones: The Variscan orogeny reconsidered. Gondwana Res. 24, 298–329.

Kryza, R., Pin, C., 2010. The Central-Sudetic ophiolites (SW Poland): Petrogenetic issues, geochronology and palaeotectonic implications. Gondwana Res. 17, 292–305.

Kurze, M., 1993. Das mittelsächsische Altpaläozoikum und seine Beziehung zu benachbarten Gebieten. Z. geol. Wiss. 20, 301–303.

Lapp, M., 1995. Strukturelle Entwicklung im weiteren Umfeld der Bohrlokation der Kontinentalen Tiefbohrung (KTB). Cuvillier Verlag, Göttingen.

Le Maitre, R.W., Streckeisen, A., Zanettin, B., Le Bas, M., Bonin, B., Bateman, P., 2005. Igneous rocks: a classification and glossary of terms: recommendations of the International Union of Geological Sciences Subcommission on the Systematics of Igneous Rocks. Cambridge University Press.

Linneman, U., Drost, K, Elicki, O., Gaitzsch, B., Gehmlich, M., Hahn, T., Kroner, U., Romer, R.L., 2008a. Das Saxothuringikum. Abriss der präkambrischen und paläozoischen Geologie von Sachsen und Thüringen. Staatliche Naturhistorische Sammlungen Dresden, Museum für Mineralogie und Geologie, Dresden.

Linneman, U., Elicki, O., Gaitzch, B., 2008b. Die stratigraphie des Saxothuringikums, In: Linneman, U. (Ed.), Das Saxothuringikum. Staatliche Naturhistorische Sammlungen Dresden, Dresden, pp. 33–74.

Linnemann, U., 2004. Das Saxothuringikum: Abriss der präkambrischen und paläozoischen Geologie von Sachsen und Thüringen; IGCP project 497 the Rheic Ozean: its origin, evolution and correlatives; unveränderter Sonderabdruck aus Geologica Saxonica (Volume 48/49). Naturhistorische Zentralbibliothek, Abt. Geowiss.

Linnemann, U., Gerdes, A., Drost, K., Buschmann, B., 2007. The continuum between Cadomian orogenesis and opening of the Rheic ocean: Constraints from LA-ICP-MS U-Pb zircon dating and analysis of plate-tectonic setting (Saxothuringian Zone, northeastern Bohemian Massif, Germany), In: Linnemann, U., Nance, R.D., Kraft, P., Zulauf, G. (Eds.), The Evolution of the Rheic Ocean: From Avalonian-Cadomian Active Margin to Alleghanian-Variscan collision. The Geological Society of Amerika, Special Paper, Boulder, Colorado, pp. 61–96.

Linnemann, U., Gerdes, A., Hofmann, M., Marko, L., 2014. The Cadomian Orogen: Neoproterozoic to Early Cambrian crustal growth and orogenic zoning along the periphery of the West African Craton—Constraints from U–Pb zircon ages and Hf isotopes (Schwarzburg Antiform, Germany). Precamb. Res. 244, 236–278.

Linnemann, U., McNaughton, N.J., Romer, R.L., Gehmlich, M., Drost, K., Tonk, C., 2004. West African provenance for Saxo-Thuringia (Bohemian Massif): Did Armorica ever leave pre-Pangean Gondwana? U/Pb-SHRIMP zircon evidence and the Nd-isotopic record. Int. J. Earth Sci. 93, 683–705.

Linnemann, U., Romer, R., Gerdes, A., Jeffries, T., Drost, K., Ulrich, J., 2010. The Cadomian orogeny in the Saxo-Thuringian zone. In: Linnemann U., Romer R.L. (Eds.), Pre-Mesozoic geology of Saxo-Thuringia: From the Cadomian active margin to the Variscan orogen. Schweizerbart, Stuttgart, pp. 37–58.

Linnemann, U, Gehmlich, M., Tichomirowa, M., Buschmann, B., Nasdala, L., Jonas, P., Luetzner, H., Bombach, K., 2000. From Cadomian subduction to early Paleozoic rifting; the evolution of Saxo-Thuringia at the margin of Gondwana in the light of single zircon geochronology and basin development (Central European Variscides, Germany). Geol. Soc.y London Spec. Publ. 179, 131–153.

Linnemann, U., Gerdes, A., Drost, K., Buschmann, B., 2007. The continuum between CAdomian orogenesis and opening of the Rheic ocean: Constraints from LA-ICP-MS U-Pb zircon dating and analysis of plate-tectonic setting (Saxothuringian Zone, northeastern Bohemian Massi, Germany), in: Linnemann, U., Nance, R.D., Kraft, P., Zulauf, G. (Eds.), The Evolution of the Rheic Ocean: From Avalonian-Cadomian Active Margin to Alleghanian-Variscan collision. The Geological Society of Amerika, Special Paper, Boulder, Colorado, pp. 61–96.

Lucassen, F., Franz, G., Kutzschbach, M., Schiperski, F., 2025. Palaeozoic high-Ti basalt, an indicator for incipient rifting, at the Saxo-Thuringian passive margin, NE-Bavaria (Germany). Int. J. Earth Sci. 114, 267–281.

Martin, U., Reischmann, T., Bahlburg, H., Schatz, M., Tait, J., Bachtadse, V., 2003. The Early Palaeozoic break-up of northern Gondwana: Sedimentology, physical volcanology and geochemistry of a submarine volcanic complex in the Bavarian facies association, Saxothuringian basin, Germany. Gondwana Res. 6, 839–858.

Martínez Catalán, J.R., Collett, S., Schulmann, K., Aleksandrowski, P., Mazur, S., 2020. Correlation of allochthonous terranes and major tectonostratigraphic domains between NW

Iberia and the Bohemian Massif, European Variscan belt. Int. J. Earth Sci. 109, 1105–1131.
Martínez Catalán, J.R., Schulmann, K., Ghienne, J. F., 2021. The Mid-Variscan Allochthon: Keys from correlation, partial retrodeformation and plate-tectonic reconstruction to unlock the geometry of a non-cylindrical belt. Earth-Science Reviews 220, 103700.
Massonne, H.J., Bautsch, H.J., 2004. Ultrahigh and high pressure rocks of Saxony, 32nd Int. Geol. Congress, Florence, Italy, p. 36.
Mazur, S., Turniak, K., Sczepanski, J., Naughton, N.J., 2015. Vestiges of Saxothuringian crust in the Central Sudetes, Bohemian Massif: Zircon evidence of a recycled subducted slab provenance. Gondwana Res. 27, 825–839.
McDonough, W.F., Sun, S. S., 1995. The composition of the Earth. Chem. Geol. 120, 223–253.
Medaris, L.G., Beard, B.L., Jelinek, E., 2006. Mantle-derived, UHP garnet pyroxentite and eclogite in the Moldanubian Gfohl nappe, Bohemian Massif: A geochemical review, new P-T determinations, and tectonic interpretation. Int. Geol. Rev.w 48, 765–777.
Mingram, B., Kroner, A., Hegner, E., Krentz, O., 2004. Zircon ages, geochemistry, and Nd isotopic systematics of pre-Variscan orthogneisses from the Erzgebirge, Saxony (Germany), and geodynamic interpretation. Int. J. Earth Sci.s 93, 706–727.
Młynarska, M., Collett, S., Anczkiewicz, R., Turniak, K., Bukała, M., Mazur, S., 2023. Vestiges of late Cambrian arc-related magmatism within the Variscan belt of Europe: Zircon geochronological and whole-rock geochemical data from the Leszczyniec Metaigneous Complex, Sudetes, Poland. Lithos 460, 107394.
Morimoto, N., 1988. Nomenclature of Pyroxenes. Mineral. Petrol.y 39, 55–76.
Murphy, J.B., Gutierrez-Alonso, G., Nance, R.D., Fernandez-Suarez, J., Keppie, J.D., Quesada, C., Dostal, J., Braid, J.A., 2009. Rheic Ocean mafic complexes: overview and synthesis. Geol. Sco. London Spec. Publ. 327, 343–369.
Murphy, J.B., Gutierrez-Alonso, G., Nance, R.D., Fernandez-Suarez, J., Keppie, J.D., Quesada, C., Strachan, R.A., Dostal, J., 2006. Origin of the Rheic Ocean: Rifting along a Neoproterozoic suture? Geology, 34, 325–328.
Murphy, J.B., Keppie, J.D., Nance, R.D., Dostal, J., 2010. Comparative evolution of the Iapetus and Rheic Oceans: A North America perspective. Gondwana Res. 17, 482–499.
Murphy, J.B., Nance, R.D., 1989. Model for the Evolution of the Avalonian-Cadomian Belt. Geology 17, 735–738.
Murphy, J.B., Nance, R.D., Mitchell, R.N., 2024. The assembly of Pangaea: geodynamic conundrums revisited. J. Geol. Soc. 181, 2024–2006.
Nance, R.D., Evans, D.A.D., Murphy, J.B., 2022. Pannotia: To be or not to be? Earth-Sci. Rev. 232, 104128.
Nance, R.D., Murphy, J.B., Strachan, R.A., Keppie, J.D., Gutierrez-Alonso, G., Fernandez-Suarez, J., Quesada, C., Linnemann, U., D'Lemos, R., Pisarevsky, S.A., 2008. Neoproterozoic-early Palaeozoic tectonostratigraphy and palaeogeography of the peri-Gondwanan terranes: Amazonian v. West African connections, Boundaries of the West African Craton. Geol. Soc. London Spec. Publ. 297, 345–383.

Nesbor, H. D., 2025. Plate tectonic relevance of intraplate and subduction-related volcanism in the Palaeozoic of the Rhenish Massif (Central Europe). Palaeobiodiversity Palaeoenviron. 105,39–60.

Neubauer, F., Liu, Y., Dong, Y., Chang, R., Genser, J., Yuan, S., 2022. Pre-Alpine tectonic evolution of the Eastern Alps: from Prototethys to Paleotethys. Earth-Sci. Rev. 226, 103923.

Nowak, I., Zelazniewicz, A., Dorr, W., Franke, W., Larionov, A.N., 2011. The Izera metabasites, West Sudetes, Poland: Geologic and isotopic U-Pb zircon evidence of Devonian extension in the Saxothuringian Terrane. Lithos 126, 435–454.

Oberc-Dziedzic, T., Kryza, R., Mochnacka, K., Larionov, A., 2010. Ordovician passive continental margin magmatism in the Central-European Variscides: U–Pb zircon data from the SE part of the Karkonosze-Izera Massif, Sudetes, SW Poland. Int. J.f Earth Sci. 99, 27–46.

Oberc-Dziedzic, T., Kryza, R., Pin, C., Mochnacka, K., Larionov, A., 2009. The orthogneiss and schist complex of the Karkonosze-Izera massif (Sudetes, SW Poland): U-Pb SHRIMP zircon ages, Nd-isotope systematics and protoliths. Geol. Sudet. 41, 3–24.

O'Brien, P., Kroner, A., Jaeckel, P., Hegner, E., Zelazniewicz, A., Kryza, R., 1997. Petrological and isotopic studies on palaeozoic high-pressure granulites, Gory Sowie Mts, Polish Sudetes. J. Petrol.y 38, 433–456.

Oliver, G.J.H., Corfu, F., Krogh, T.E., 1993. U-Pb ages from SW Poland: evidence for a Caledonian suture zone between Baltica nad Gondwana. J. Geol. Soc.y 147, 355–369.

Patočka, F., Dostal, J., Pin, C., 1997. Early Palaeozoic intracontinental rifting in the central west Sudetes, Bohemian Massif: geochemical and Sr–Nd isotopic study on felsic-mafic meta-volcanics of the Rychory Mts Complex, Terra Nova Abstr Suppl, 144–145.

Patočka, F., Fajst, M., Kachlík, V., 2000. Mafic-felsic to mafic-ultramafic Early Palaeozoic magmatism of the West Sudetes (NE Bohemian Massif): the South Krkonoše Complex. Z. geol. Wiss. 28, 177–210.

Patočka, F., Pin, C., 2005. Sm-Nd isotope and trace element evidence for heterogeneous igneous protoliths of Variscan mafic blueschists in the East Krkonoše Complex (West Sudetes, NE Bohemian Massif, Czech Republic). Geodinam. Acta 18, 363–374.

Patočka, F., Štorch, P., 2004. Evolution of geochemistry and depositional settings of Early Palaeozoic siliciclastics of the Barrandian (Tepla-Barrandian Unit, Bohemian Massif, Czech Republic). Int. J. Earth Sci. 93, 728–741.

Patočka, F., Vlašímský, P., Blechová, K., 1993. Geochemistry of Early Paleozoic volcanics of the Barrandian basin (Bohemian Massif, Czech Republic): implications for paleotectonic reconstructions. Jb. geol. Bundesanst. 136, 873–896.

Pearce, J.A., Wyman, D., 1996. A user's guide to basalt discrimination diagrams. Trace element geochemistry of volcanic rocks: applications for massive sulphide exploration. Geol.l Assoc. Canada, Short Course Notes 12, 113.

Perraki, M., Faryad, S.W., 2014. First finding of microdiamond, coesite and other UHP phases in felsic granulites in the Moldanubian Zone: Implications for deep subduction and a revised geodynamic model for Variscan Orogeny in the Bohemian Massif. Lithos 202, 157–166.

Pin, C., Kryza, R., Oberc-Dziedzic, T., Mazur, S., Turniak, K., Waldhausrová, J., 2007. The diversity and geodynamic significance of Late Cambrian (ca. 500 Ma) felsic anorogenic magmatism in the northern part of the Bohemian Massif: A review based on Sm-Nd isotope and geochemical data. Geol. Soc. Amer. Spec. Publ. 423, 209–230.

Rapprich, V., 2005. Compositional variation of clinopyroxenes of basaltic, essexitic and tephriphonolitic rocks from the Doupovské hory Volcanic Complex, NW Bohemia. J Czech Geol. Soc. 50, 119–132.

Rapprich, V., Lisec, M., Fiferna, P., Závada, P., 2017. Application of modern technologies in popularization of the Czech volcanic geoheritage. Geoheritage 9, 413–420.

Romer, R.L., Hahne, K., 2010. Life of the Rheic Ocean: scrolling through the shale record. Gondwana Res. 17, 236–253.

Rötzler, J., Timmerman, M.J., 2021. Geochronological and petrological constraints from the evolution in the Saxon Granulite Massif, Germany on the Variscan continental collision orogeny. J. Metam. Geol. 39, 3–38.

Salamon, M., Königshof, P., 2010. Middle Devonian olistostromes in the Rheno-Hercynian zone (Rheinisches Schiefergebirge)—an indication of back arc rifting on the southern shelf of Laurussia. Gondwana Res. 17, 281–291.

Schmädicke, E., Will, T.M., Ling, X., Li, X.-H., Li, Q. L., 2018. Rare peak and ubiquitous post-peak zircon in eclogite: Constraints for the timing of UHP and HP metamorphism in Erzgebirge, Germany. Lithos 322, 250–267.

Schulmann, K., Edel, J. B., Martínez Catalán, J.R., Mazur, S., Guy, A., Lardeaux, J. M., Ayarza, P., Palomeras, I., 2022. Tectonic evolution and global crustal architecture of the European Variscan belt constrained by geophysical data. Earth-Sci. Rev. 234, 104195.

Schulmann, K., Lexa, O., Stipska, P., Racek, M., Tajcmanova, L., Konopasek, J., Edel, J.B., Peschler, A., Lehmann, J., 2008. Vertical extrusion and horizontal channel flow of orogenic lower crust: key exhumation mechanisms in large hot orogens? J. Metam. Geol. 26, 273–297.

Siebel, W., Raschka, H., Irber, W., Kreuzer, H., Lenz, K.L., Hohndorf, A., Wendt, I., 1997. Early palaeozoic acid magmatism in the Saxothuringian belt: New insights from a geochemical and isotopic study of orthogneisses and metavolcanic rocks from the Fichtelgebirge, SE: Germany. J. Petrol. 38, 203–230.

Štědrá, V., Kachlík, V., Kryza, R., 2002. Coronitic metagabbros of the Mariánské Lázně Complex and Teplá Crystalline Unit: inferences for the tectonometamorphic evolution of the western margin of the Teplá Barrandian Unit, Bohemian Massif. Geol. Soc. London Spec. Publ. 201, 217–236.

Sun, S.S., McDonough, W.F., 1989. Chemical and isotopic systematic of oceanic basalts: Implication for mantle composition and processes. Geol. Soc. London Spec. Publ. 42, 313–345.

Syahputra, R., Žák, J., Tomek, F., Kachlík, V., 2023. Hot plutonism in a cold accretionary wedge: What terminated the Cadomian orogeny along the northern periphery of Gondwana? Precamb. Res. 390, 107041.

Tasáryová, Z., Janoušek, V., Frýda, J., 2018. Failed Silurian continental rifting at the NW margin of Gondwana: evidence from basaltic volcanism of the Prague Basin (Teplá–Barrandian Unit, Bohemian Massif). Int. J. Earth Sci. 107, 1231–1266.

Timmermann, H., Stedra, V., Gerdes, A., Noble, S.R., Parrish, R.R., Dorr, W., 2004. The problem of dating high-pressure metamorphism: A U-Pb isotope and geochemical study on eclogites and related rocks of the Marianske Lazne Complex, Czech Republic. J. Petrol. 45, 1311–1338.

Tracy, R., Robinson, P., 1977. Zoned titanian augite in alkali olivine basalt from Tahiti and the nature of titanium substitutions in augite. Amer. Mineral.t 62, 634–645.

Villa, I.M., Holden, N.E., Possolo, A., Ickert, R.B., Hibbert, D.B., Renne, P.R., Bonardi, M.L., De Bievre, P., 2022. IUGS–IUPAC recommendations and status reports on the half-lives of ^{87}Rb, ^{146}Sm, ^{147}Sm, ^{234}U, ^{235}U, and ^{238}U (IUPAC Technical Report). Pure Appl. Chem. 94, 1085–1092.

Van Staal, C.R., Dewey, J.F., Mac Niocaill, C., Mc Kerrow, W.S., 1998. Cambrian-Silurian tectonic evolution of the northern Appalachians and British Caledonides: history of a complex, west and southwest Pacific type segment of Iapetus, in: Blundell, D.J., Scott, A.C. (Eds.), Lyell; the past is the key to present. Geol. Soc. London, Spec. Publ., pp. 199–242.

Vermeesch, P., 2018. IsoplotR: A free and open toolbox for geochronology, Geosci. Front., 9, 1479–1493.

von Raumer, J.F., Stampfli, G.M., 2008. The birth of the Rheic Ocean - Early Palaeozoic subsidence patterns and subsequent tectonic plate scenarios. Tectonophysics 461, 9–20.

Whitney, D.L., Evans, B.J., 2010. Abbreviation for names of rock-forming minerals. Amer. Mineral.t 95, 185–187.

Willner, A.P., Krohe, A., Maresch, M.V., 2000. Interrelated P-T-t-d paths in the Variscan Erzgebirge dome (Saxony, Germany): Constraints on the rapid exhumation of high-pressure rocks from the root zone of a collisional orogen. Int. Geol. Rev. 42, 64–85.

Winchester, J.A., Floyd, P.A., Crowley, Q.G., Piasecki, M.A.J., Lee, M.K., Pharaoh, T.C., Williamson, P., Banka, D., Verniers, J., Samuelsson, J., Bayer, U., Marotta, A.M., Lamarche, J., Franke, W., Dörr, W., Valverde-Vaquero, P., Giese, U., Vecoli, M., Thybo, H., Laigle, M., Scheck, M., Maluski, H., Marheine, D., Noble, S.R., Paarish, R.R., Evans, J., Timmerman, H., Gerdes, A., Guterch, A., Grad, M., Cwojdzinski, S., Cymerman, Z., Kozdroj, W., Kryza, R., Alexandrowski, P., Mazur, S., Stedrá, V., Kotková, J., Belka, Z., Patoćka, F., Kachlik, V., 2002. Palaeozoic amalgamation of Central Europe: New results from recent geological and geophysical investigations. Tectonophysics 360, 5–21.

Wood, D.A., 1980. The application of a Th-Hf-Ta diagram to problems of tectomagmatic classification and to establishing the nature of crustal contamination of basaltic lavas of the British Tertiary volcanic province. Earth Planet. Sci. Lett. 50, 11–30.

Workman, R.K., Hart, S.R., 2005. Major and trace element composition of the depleted MORB mantle (DMM). Earth Planet. Sci. Lett. 231, 53–72.

Zak, J., Kraft, P., Hajna, J., 2013. Timing, styles, and kinematics of Cambro-Ordovician extension in the Tepla-Barrandian Unit, Bohemian Massif, and its bearing on the opening of the Rheic Ocean. Int. J. Earth Sci.s 102, 415–433.

Žák, J., Sláma, J., 2018. How far did the Cadomian ʻterranes' travel from Gondwana during early Palaeozoic? A critical reappraisal based on detrital zircon geochronology. Int. Geol. Rev. 60, 319–338.

Žák, J., Sláma, J., Syahputra, R., Nance, R.D., 2023. Dynamics of Cambro–Ordovician rifting of the northern margin of Gondwana as revealed by the timing of subsidence and magmatism in rift-related basins. Int. Geol. Rev. 65, 3004–3027.

Žák, J., Verner, K., Sláma, J., Kachlík, V., Chlupáčová, M., 2013. Multistage magma emplacement and progressive strain accumulation in the shallow-level Krkonoše–Jizera plutonic complex, Bohemian Massif. Tectonics 32, 1493–1512.

Zartman, R.E., Doe, B.R., 1981. Plumbotectonics—the model. Tectonophys. 75, 135–162.

Zeh, A., Bratz, H., Millar, I.L., Williams, I.S., 2002. A combined zircon SHRIMP and Sm-Nd study of high-grade paragneisses from the Mid-German Crystalline Rise: evidence for northern Gondwanan and Grenvillian provenance. J. Geol. Soc. 159, 1–3.

Zeh, A., Gerdes, A., 2010. Baltica and Gondwana-derived sediments in the Mid-German Crystalline Rise (Central Europe): Implications for the closure of the Rheic ocean. Gondwana Res. 17, 254–263.

Żelaźniewicz, A., Dörr, W., Bylina, P., Franke, W., Haack, U., Heinisch, H., Schastok, J., Grandmontagne, K., Kulicki, C., 2004. The eastern continuation of the Cadomian orogen: U–Pb zircon evidence from Saxo-Thuringian granitoids in south-western Poland and the northern Czech Republic. Int. J. Earth Sci. 93, 773–781.

Figures with captions:

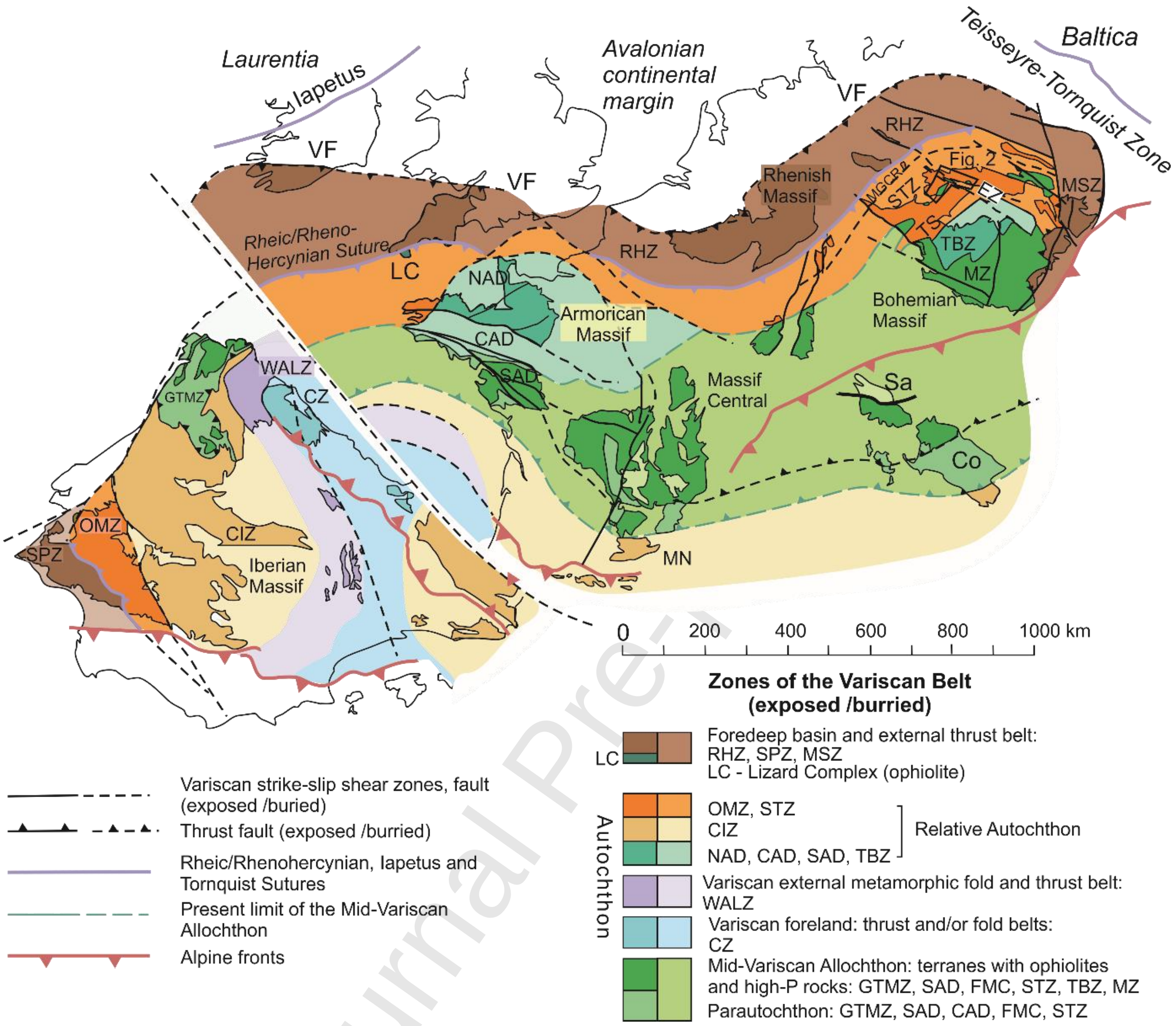

Figure 1

Late Paleozoic reconstruction of the Variscan orogen and assumed sutures of the closed early Paleozoic oceanic tract of Western and Central Europe (slightly modified after Schulmann et al. 2022). Zones of the Variscan Belt: CZ, Cantabrian; CIZ, Central Iberian: GTMZ, Galicia-Trás-os-Montes; MSZ, Moravo-Silesian Zone; MZ- Moldanubian Zone; OMZ, Ossa-Morena Zone; RHZ, Rhenohercynian Zone; SPZ, South Portuguese Zone; STZ, Saxothuringian Zone; TBZ, Teplá-Barrandian Zone; WALZ, West Asturian-Leonese Zone; Other abbreviation: NAD, North, CAD, Central, SAD, South Armorican Domains: Co, Corsica; LC, Lizard Complex; MGCR, Mid-German Crystalline Rise; MN, Montagne Noire; MTM, Maures/Tanneron Massif; VM, Vosges Massif; SWM, Schwarzwald Massif; TS, Teplá Suture); VF, Variscan Front; EFZ, Elbe fault Zone.

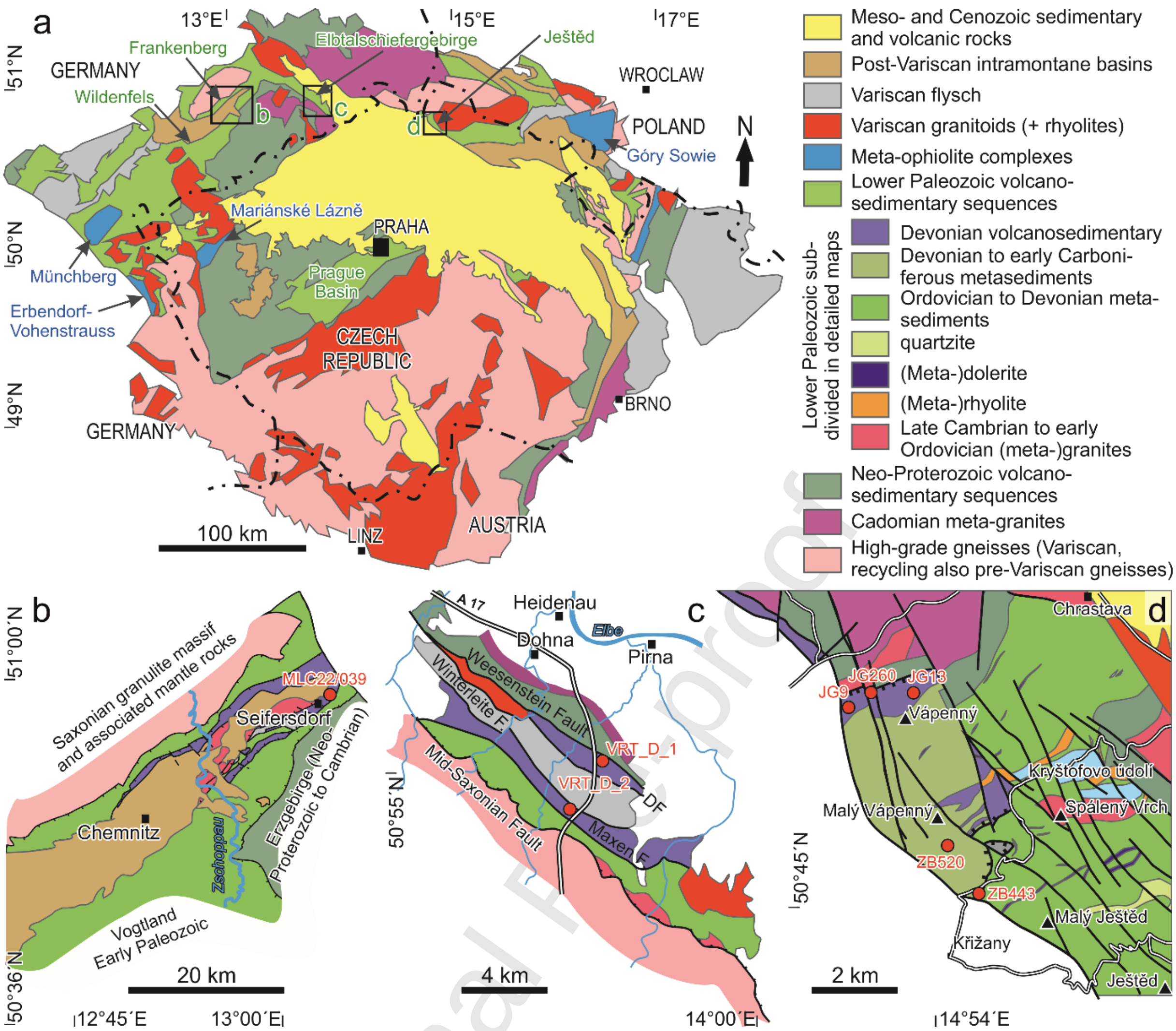

Figure 2

Location of study areas: (a) Simplified geological map of the Bohemian Massif with individual sampling areas indicated (modified after Martínez Catalán et al., 2021); (b) Simplified geological map of the Frankenberg klippe (adopted from geological map 1:200 000 CC5542 Dresden Berger H. J. (2001) and location of the Seifersdorf quarry (samples MLC22/039a,b,c,d); (c) Simplified geological map of the Elbtalschiefergebirge (adopted from Königshof and Linnemann, 2008) with location of VRT_D_1 and VRT_D_2 boreholes; (d) Simplified geological map of the Ještěd Mts. (simplified from an unpublished map made by V. Kachlík) with location of analyzed samples.

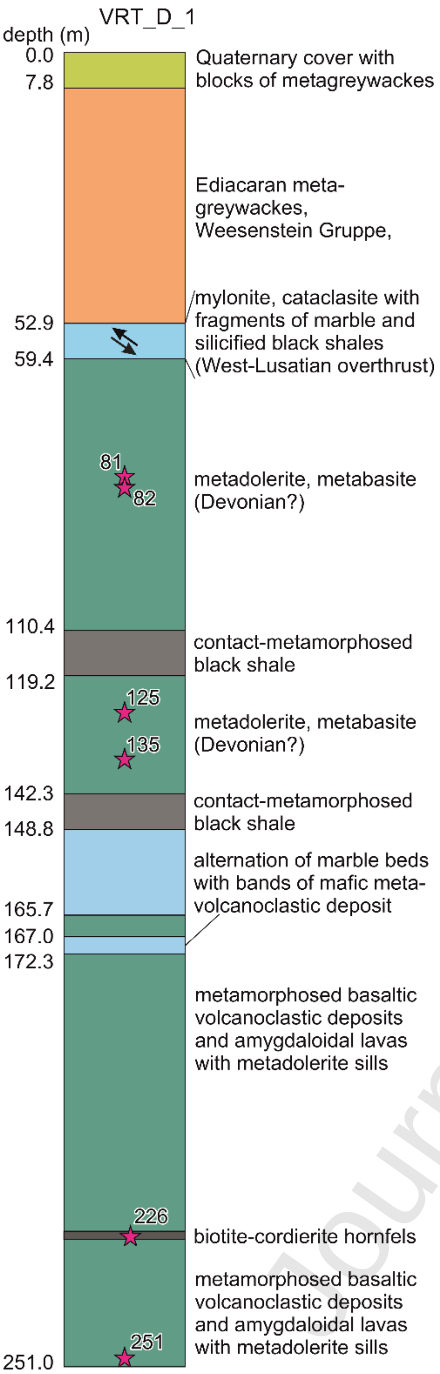

Figure 3

Lithological drill-log of the VRT_D_1 drill-core. Position of analyzed samples is indicated by stars.

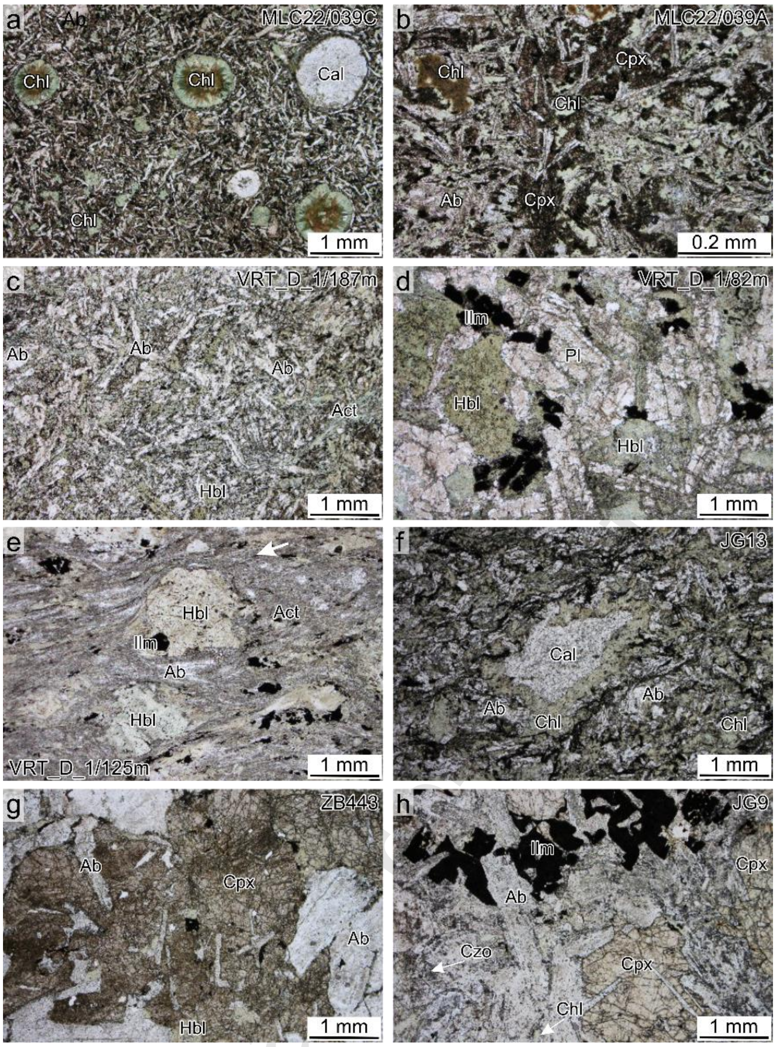

Figure 4

Petrography of studied rocks (all microphotographs in plane-polarized light). Frankenberg klippe: a – amygdaloidal lava with chlorite- and calcite-filled vesicles (MLC22/039C); b – dolerite from feeding dyke (MLC22/039A); Elbtalschiefergebirge (borehole VRT_D_1); c – fine-grained metadolerite with euhedral laths of albite and fine grained matrix composed of chlorite, actinolite and ilmenite; d –medium- to coarse-grained metadolerite with ferrohornblede to actinolite completely replacing former pyroxene and broken grains of magmatic ilmenite, partly leucoxenized at margins; e – rotated porphyroclast of hornblende in fine-grained and recrystallized matrix composed of albite, chlorite and ilmenite; Ještěd Mts.: f –zoned amygdales filled by calcite with chlorite rim in recrystallized fine-grained matrix in lava metamorphosed at greenschist conditions, with albite laths after former basic feldspar and disseminated ilmenite; g – coarse-grained metadolerite with preserved augite and albitized plagioclase; h - skeletal magmatic ilmenite and augite in medium-grained metadolerite with greenschist facies minerals in the matrix. Ab – albite, Act – actinolite, Cal – calcite, Chl – chlorite, Cpx – clinopyroxene, Czo – clinozoisite, Hbl – hornblende, Ilm – ilmenite, Pl – plagioclase. Mineral abbreviations are after Whitney and Evans (2010).

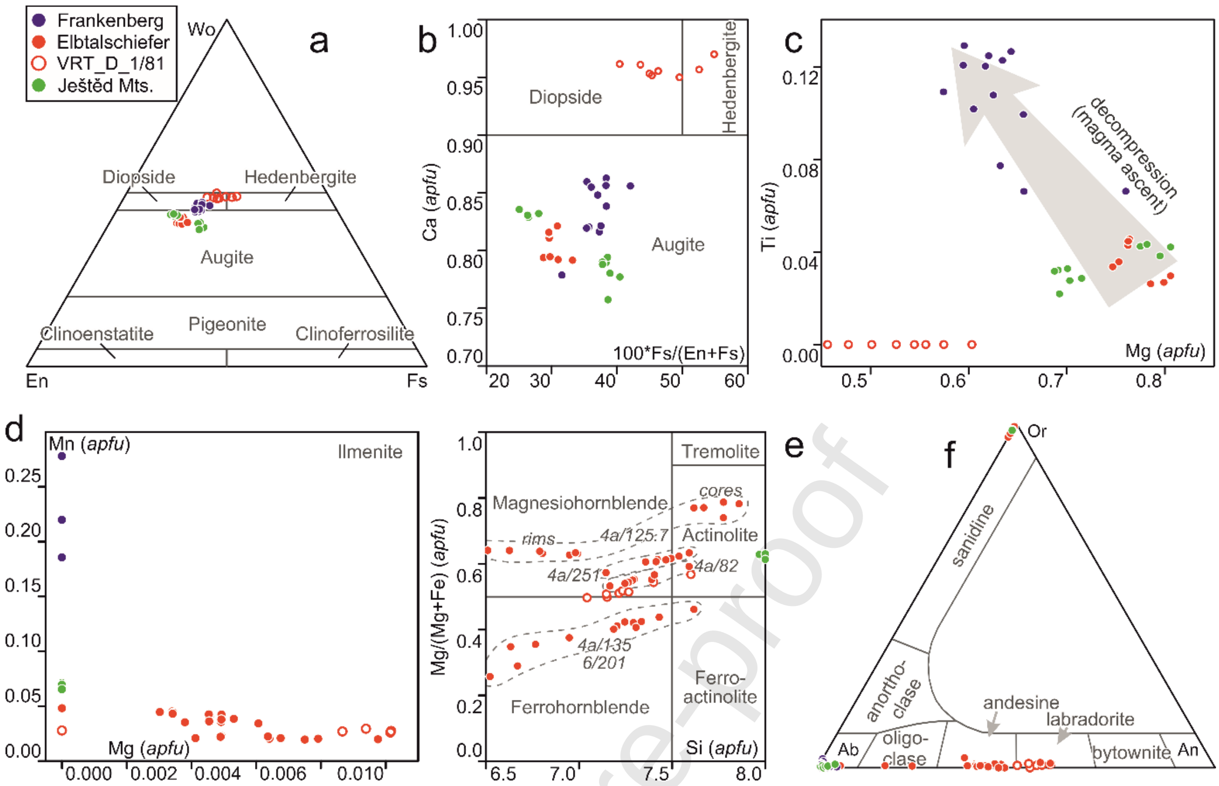

Figure 5

Mineral chemistry: a – quadrilateral classification diagram of pyroxenes (Morimoto, 1988); b – orthogonal projection of pyroxene composition avoiding tschermak-substitution effect (Rapprich, 2005); c – Mg *vs.* Ti (*apfu*) binary diagram for analyzed clinopyroxenes; d – Mg *vs.* Mn (*apfu*) binary diagram for analyzed ilmenites; e – classification diagram of amphiboles (Leake et al., 1997); f – classification diagram of feldspars.

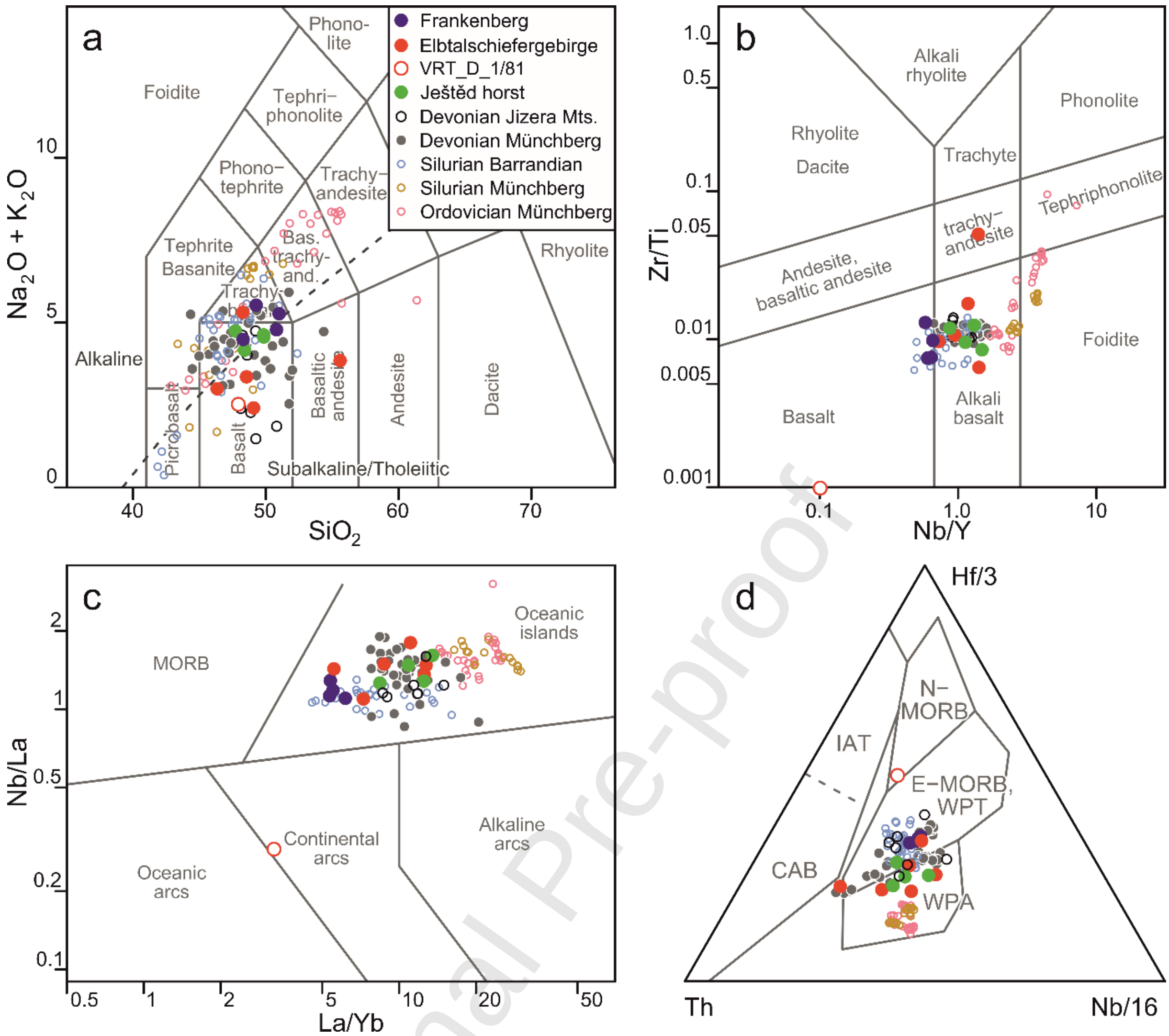

Figure 6

Bulk-rock classification: a – Total alkali silica “TAS” classification diagram” (LeMaitre et al., 2002); b – Zr/Ti vrs. Nb/Y classification diagram (Pearce, 1996); c – Nb/La vs. La/Yb geotectonic diagram (Hollocher et al., 2012); d – Th–Hf/3–Nb/16 geotectonic discrimination ternary plot (Wood,1980). Data on Ordovician, Silurian, and Devonian alkali-basaltic rocks from the allochthonous units of the Münchberg klippe (MK), as well as the underlying Thuringian parautochthon, are sourced from Höhn et al. (2018) and Koglin et al. (2017). Data from Prague Basin (PB) are sourced from Tasáryová et al. (2018). Additionally, Devonian alkali-basaltic dykes that intrude Jizera orthogneiss (JO) are taken from publication by Nowak et al. (2011).

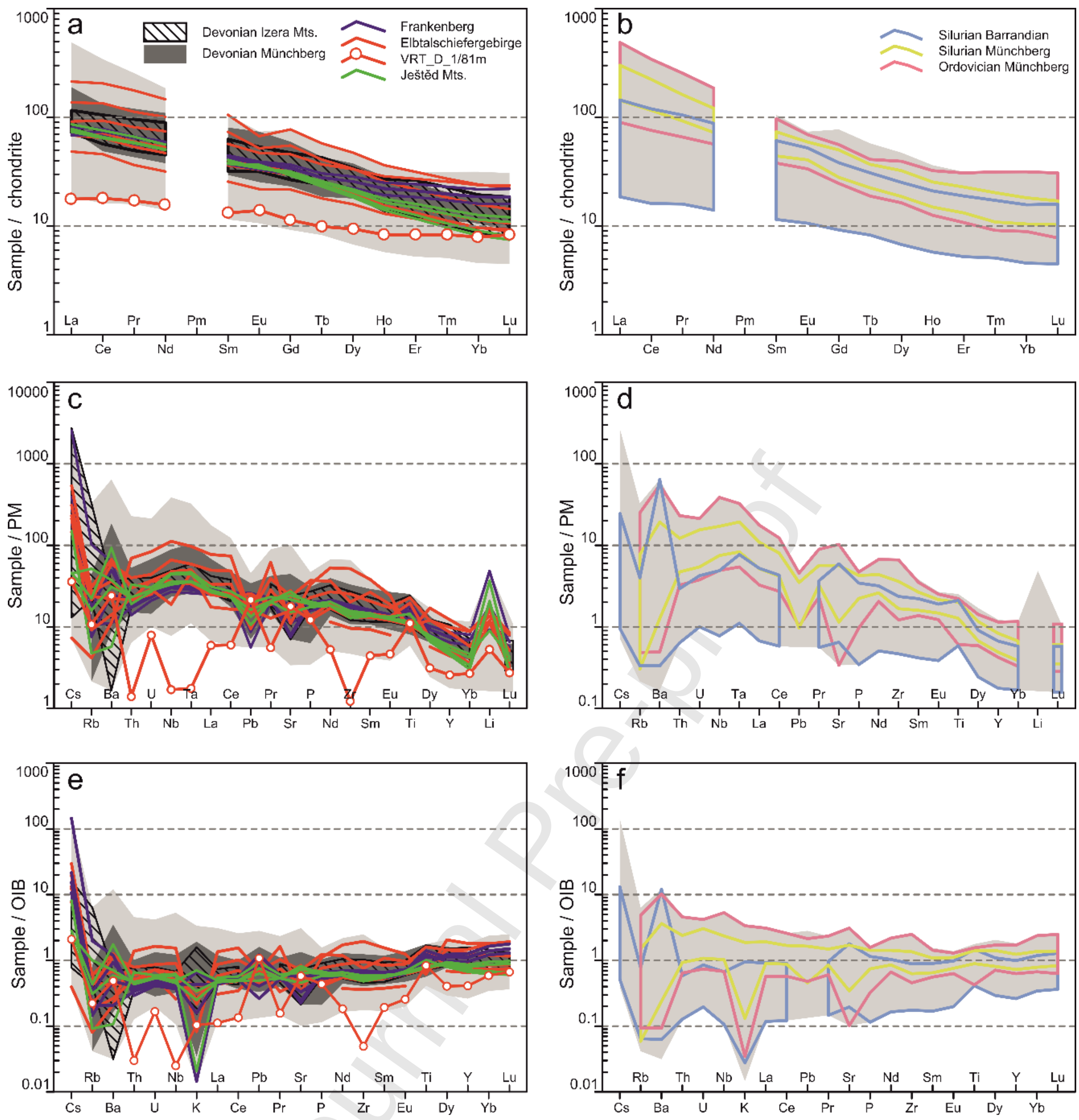

Figure 7

Spider plots for the studied Devonian basalts of the allochthonous units of the Frankenberg klippe, the Elbetalchiefergebirge, and the Ještěd Mts., and their comparison with Devonian basalts intruding JO, Devonian basalts of Prasinite–Phyllite "Series", Devonian basalts of the parautochthonous Thuringian facies (TF) in the vicinity of the Münchberg Klippe (MK) and Silurian basalts of the PB. Spider plots: a – normalized to CI chondrite (Anders and Grevesse, 1989); b – normalized to Primitive Mantle (McDonough and Sun, 1995); c – normalized to ocean island basalt (Sun and McDonough, 1989). The grey shaded field represents Ordovician and Silurian basalts from the footwall of MK and its basal allochthonous part.; c,d,e – Compositional ranges for Ordovician and Silurian basalts of the above-mentioned units of MK and parautochthonous Thuringian facies (TF) units adjacent to MK and for the Silurian of the Prague Basin. Samples are normalized as in a, b, c. Data sources are the same as in Figure 6.

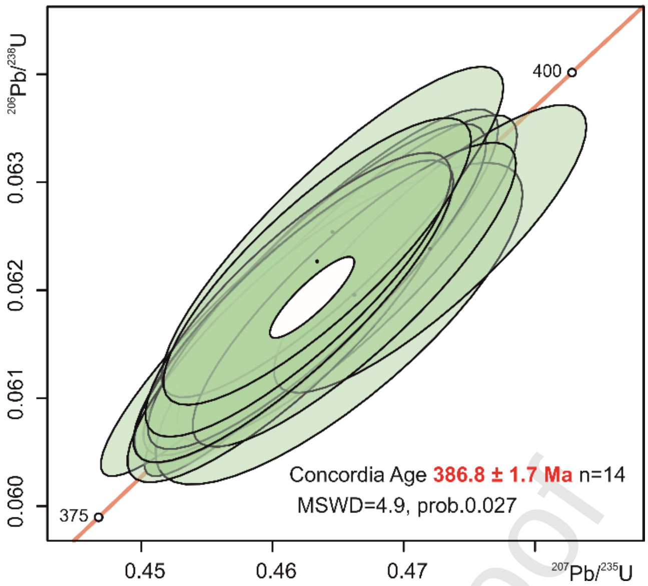

Figure 8

Concordia age plot of U–Pb zircon analyses from metarhyolite ZB-520 sample (see petrographic description in ESM 2, U–Pb zircon analyses and ages are given ESM 5). Age calculated using Isoplot R software (Vermeesch, 2018).

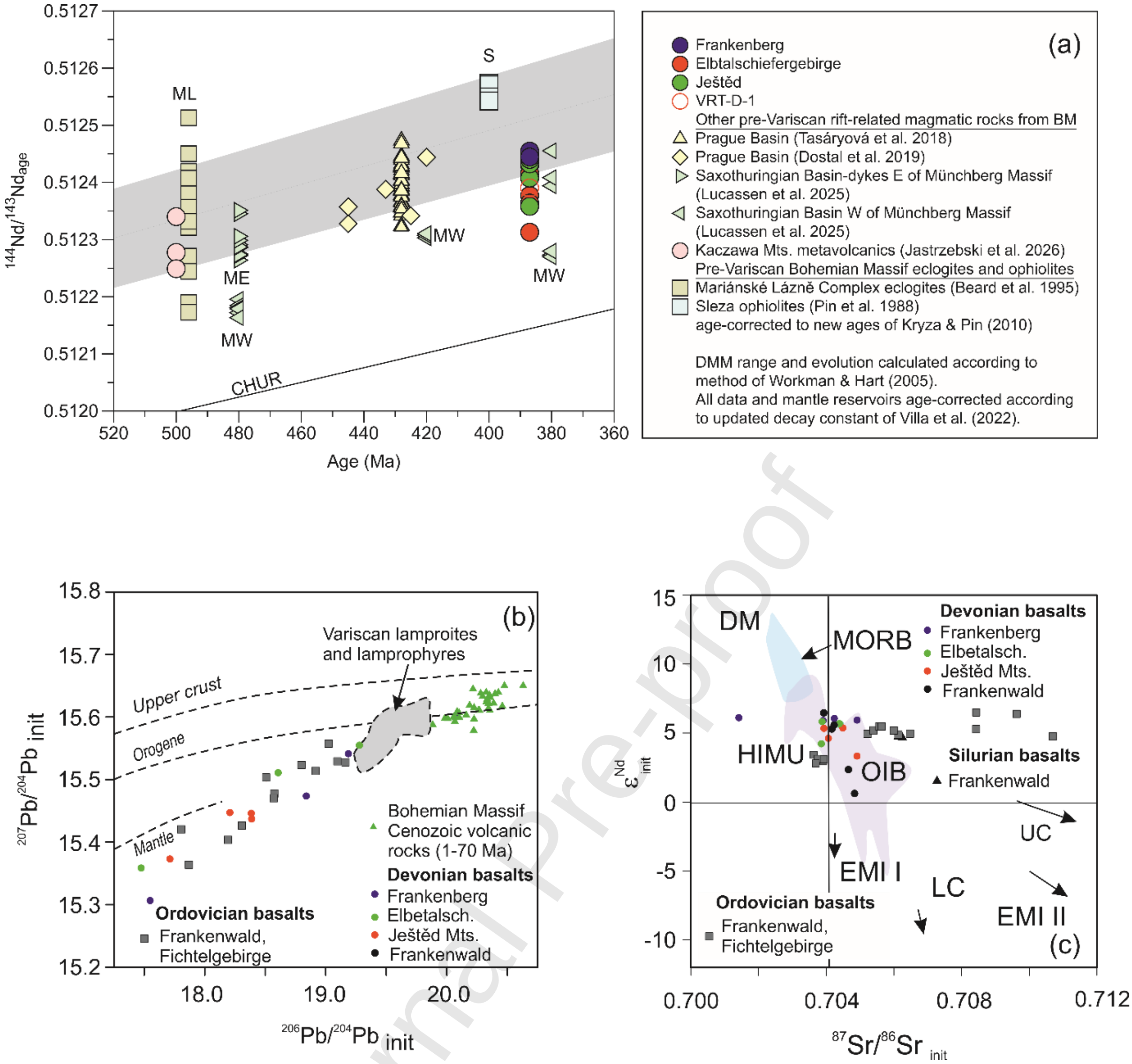

Figure 9

The Sr–Nd–Pb isotope composition of Devonian rift-related metabasalts from Frankenberg, Elbetalschiefergebirge and Ještěd Mts. Units (this study) compared with published data from other autochthonous and allochthonous Ordovician to Devonian units of Saxothuringian Zone and adjacent Teplá–Barrandian Unit): a) plot of age versus $^{144}Nd/^{143}Nd_{(i)}$ of Ordovician to Devonian rift-related (meta)basaltic rocks and associated MORB-like metabasalts from the Saxothuringian Zone, Teplá–Barrandian Unit and Teplá and Rheic suture (Ślęża ophiolite); b) Plot of $^{206}Pb/^{204}Pb_i$ vs $^{207}Pb/^{204}Pb_i$ of studied Devonian metabasalts and their comparison with Ordovician rift-related basalts and Varsican lamprophyres showing differences caused by different mantle sources and assimilation/fractionation processes. Data for Ordovician basalts from autochthonous and allochthonous units underlying MK are from Lucassen et al. (2025), data for Variscan lamprophyre dykes are from Krmíčková et al. (2020). Evolution lines of upper crustal and orogenic rocks are from Zartman and Doe (1981).

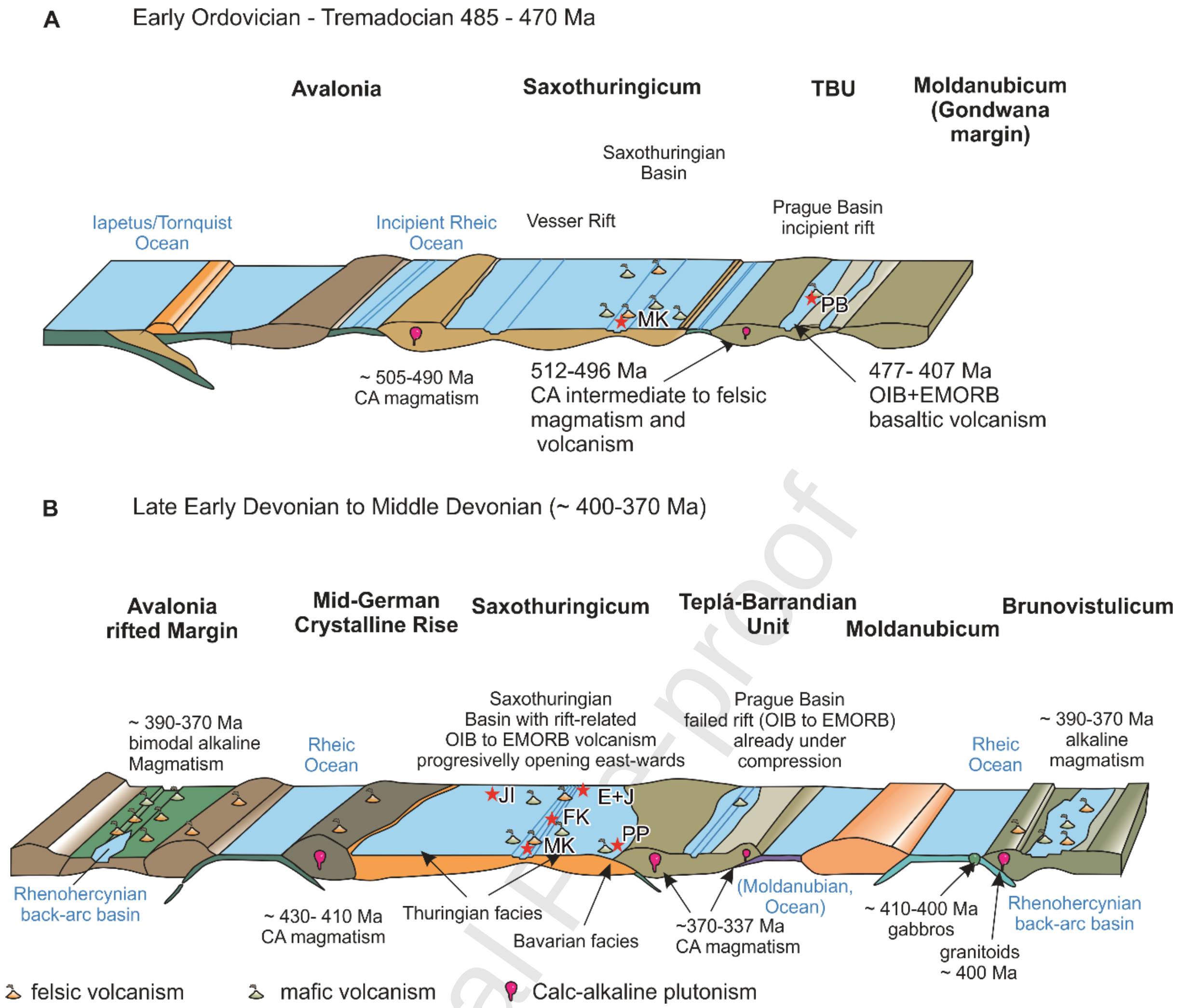

Figure 10

Plate tectonic model of recurrent (Ordovician to Devonian) rifting of the Saxothuringian Zone and adjacent units: a) Early Ordovician-Tremadocian (485–470 Ma), b) Late Early Devonian to Middle Devonian time span (~ 400–370 Ma). Note that the Rheic Ocean appears twice due to oroclinal bending in the Bohemian Massif.

Table 1: Major and trace element chemistry of samples from this study

	MLC22/039A	MLC22/039B	MLC22/039C	MLC22/039D	VRT_D1/81	VRT_D1/82	VRT_D1/125.7	VRT_D1/135	VRT_D1/226	VRT_D1/251	VRT_D2/201	JG-9	JG-13	JG-260	ZB-443
Si	44.	47.	44.	48.	47.02	44.97	47.58	54.21	57.02	46.81	46.04	48	42.	46	47
Ti	2.5	3.1	3.5	4.0	2.39	3.94	2.03	1.77	0.76	2.13	4.60	2.	2.2	2.	2.
Al	15.	12.	10.	11.	13.49	13.98	10.89	14.45	20.17	13.48	11.80	14	12.	14	14
Fe	1.9	2.6	2.2	5.2	4.85	0.64	2.30	1.42	0.59	0.61	2.14	3.	5.1	4.	3.
Fe	8.7	8.7	10.	7.2	5.08	11.44	11.86	8.23	7.02	9.60	9.84	7.	6.1	7.	7.
M	0.1	0.1	0.4	0.3	0.17	0.16	0.18	0.15	0.02	0.24	0.20	0.	0.1	0.	0.
M	7.3	5.6	4.6	4.4	6.48	7.49	12.73	6.33	1.42	7.74	5.98	5.	6.0	7.	5.
C	7.2	7.2	8.7	8.8	15.84	11.24	6.27	6.51	0.36	12.34	9.25	9.	9.5	9.	8.
N	3.9	4.3	4.0	4.5	2.30	2.43	2.03	3.63	0.41	2.63	4.69	4.	4.1	2.	3.
K_2	0.2	0.6	0.9	0.0	0.15	0.48	0.31	0.12	7.32	0.61	0.38	0.	0.0	1.	0.
P_2	0.3	0.4	0.3	0.3	0.27	0.28	0.76	0.68	0.07	0.25	0.47	0.	0.3	0.	0.
F	0.0	0.0	0.1	0.1	0.05	0.07	0.06	0.10	0.05	0.06	0.07	n.	n.a	n.	n.
C	0.5	1.5	3.4	0.9	0.23	0.28	0.02	0.16	0.02	0.94	0.61	0.	7.1	0.	0.
S	0.0	0.1	0.0	0.1	bdl	bdl	bdl	0.42	0.03	0.25	0.15	n.	n.a	n.	n.
H_2	5.1	3.5	4.0	2.5	0.95	1.61	2.32	1.94	3.99	1.60	2.78	2.	4.2	3.	3.
L	0.2	0.3	0.3	0.1	0.05	0.06	0.16	0.11	0.27	0.09	0.20	0.	0.3	0.	0.
T	99.	99.	99.	99.	99.44	99.15	99.60	100.1	99.63	99.41	99.22	99	10	99	99
Li	77.	29.	14.	18.	9.10	18.1	19.1	21.5	77.0	29.2	25.0	14	58.	33	32
Sc	38.	42.	36.	41.	32.3	33.8	15.6	12.9	15.3	27.2	49.0	38	23.	20	25
V	376	481	469	537	203	362	217	72.5	149	264	570	32	25	22	28
Cr	184	39.	42.	49.	410	164	593	4.40	103	213	22.0	59	39	22	71
C	41.	38.	39.	45.	41.5	47.9	80.2	24.1	14.7	38.2	34.8	38	47.	41	36
Ni	78.	28.	31.	35.	96.8	117	420	3.41	74.8	80.2	17.7	37	26	10	93
C	56.	56.	25.	59.	48.0	74.0	9.35	30.5	72.1	91.1	32.6	69	73.	53	10
Z	97.	109	114	103	101	115	143	220	120	104	116	11	93.	11	11
G	22.	19.	16.	19.	18.4	20.7	19.2	29.9	26.5	20.9	23.3	22	19.	23	22
R	4.4	10.	61.	6.4	6.93	16.1	12.9	2.50	224	18.4	14.2	9.	2.8	31	13
Sr	370	160	219	149	382	554	469	219	73.35	533	288	30	43	48	54
Y	36.	31.	27.	32.	11.9	22.2	36.9	52.7	22.2	25.2	42.4	24	22.	20	19
Zr	195	187	161	180	13.8	152	212	544	91.9	136	266	15	16	13	14
N	21.	20.	17.	19.	1.20	31.4	43.5	73.8	16.7	23.9	30.7	21	29.	23	28
M	0.7	0.5	1.1	0.5	0.10	1.17	2.22	3.96	0.17	0.79	1.27	0.	0.0	0.	0.
C	0.1	0.1	0.1	0.3	0.13	0.18	0.19	0.42	0.10	0.16	0.18	0.	0.1	0.	0.
Sn	1.5	1.2	1.5	1.3	0.69	1.81	1.10	1.51	2.93	1.77	1.61	1.	2.1	1.	3.
Sb	3.2	2.5	0.1	0.1	0.12	3.06	1.00	2.20	0.20	2.26	0.75	0.	19.	2.	1.
Cs	4.1	8.3	56.	5.9	0.81	11.5	3.00	0.15	24.8	4.77	7.59	0.	3.1	0.	1.
B	169	327	416	72.	171	240	389	74.6	748	443	147	20	37.	24	61
La	18.	16.	16.	16.	4.13	17.4	32.1	50.0	40.0	16.0	21.5	17	20.	18	18
C	47.	44.	40.	44.	10.8	42.7	81.2	124	87.2	39.0	56.3	38	45.	39	39
Pr	5.9	5.7	5.0	5.7	1.52	5.31	10.0	15.7	8.87	4.76	7.23	5.	5.9	5.	5.
N	26.	26.	22.	26.	7.08	24.1	45.6	66.2	32.9	21.2	33.7	22	25.	22	23
S	6.5	6.2	5.4	6.3	1.93	5.93	10.8	15.5	6.01	5.31	8.38	5.	5.9	5.	5.
E	2.1	2.0	1.8	2.0	0.77	2.05	2.91	3.76	1.37	1.84	2.63	1.	1.9	1.	2.
G	7.2	6.6	5.9	6.8	2.21	6.13	10.8	15.2	5.65	5.80	8.99	6.	6.2	5.	5.
T	1.1	1.0	0.8	1.0	0.36	0.87	1.49	2.09	0.76	0.85	1.34	0.	0.9	0.	0.
D	6.9	6.2	5.4	6.2	2.27	4.85	8.17	11.5	4.34	4.99	8.09	5.	5.0	4.	4.
H	1.3	1.2	1.0	1.2	0.46	0.86	1.42	2.02	0.82	0.92	1.59	0.	0.9	0.	0.
Er	3.8	3.3	2.9	3.3	1.32	2.11	3.46	5.01	2.26	2.33	4.32	2.	2.3	2.	1.
T	0.5	0.4	0.4	0.4	0.20	0.27	0.44	0.66	0.33	0.31	0.62	0.	0.3	0.	0.
Y	3.5	3.0	2.6	3.0	1.27	1.57	2.56	3.92	2.17	1.84	3.87	2.	1.8	1.	1.
L	0.5	0.4	0.3	0.4	0.20	0.22	0.35	0.54	0.33	0.26	0.58	0.	0.2	0.	0.
Hf	4.4	4.2	3.6	4.0	0.54	3.82	4.86	11.7	2.35	3.28	6.00	3.	4.0	3.	3.
Ta	1.1	1.1	0.9	1.0	0.07	1.85	2.18	3.60	0.88	1.24	1.61	1.	1.7	1.	1.
W	0.1	0.1	0.1	0.0	0.09	0.42	0.31	0.50	1.42	0.43	0.67	0.	0.8	0.	0.

Tl	bdl	bdl	0.3	0.0	bdl	0.042	0.086	0.038	0.97	0.089	0.15	0.	0.0	0.	1.
Pb	2.6	3.8	0.8	1.3	3.45	2.48	2.19	2.19	14.6	3.83	1.42	1.	2.9	2.	2.
T	1.6	1.4	1.1	1.3	0.12	1.73	3.15	5.53	12.3	2.38	2.00	1.	2.6	1.	1.
U	0.5	0.5	0.4	0.4	0.17	0.50	0.88	1.67	1.04	0.73	0.74	0.	0.6	0.	0.

Contents of major elements are given in wt.%; concentrations of trace elements are given in ppm.

bdl – below detection limit; n.a. – not analyzed; LOI – crystalline water

Table 2: Strontium, Nd and Pb isotope compositions of samples from this study

	$^{87}Sr/^{86}Sr$	$^{87}Sr/^{86}Sr_{(i)}$	$^{143}Nd/^{144}Nd$	$^{143}Nd/^{144}Nd_{(i)}$	εN	T_{DM}	T_{DM} 2stg	$^{206}Pb/^{204}Pb$	$^{206}Pb/^{204}Pb_{(i)}$	$^{207}Pb/^{204}Pb$	$^{207}Pb/^{204}Pb_{(i)}$	$^{208}Pb/^{204}Pb$	$^{208}Pb/^{204}Pb_{(i)}$
MLC22/	0.705	0.704	0.5128	0.51244	5.	0.7	0.61	19.09	16.679	15.60	15.474	38.77	38.513
MLC22/	0.705	0.704	0.5128	0.51245	6.	0.6	0.61	18.85	17.373	15.62	15.541	38.69	38.531
MLC22/	0.705	0.701	0.5128	0.51245	6.	0.6	0.60						
MLC22/	0.704	0.703	0.5128	0.51244	5.	0.7	0.62	19.74	18.304	15.61	15.535	39.00	38.541
VRT_D1	0.703	0.703	0.5128	0.51238	4.	0.9	0.70	18.54	18.343	15.64	15.634	38.74	38.681
VRT_D1	0.704	0.704	0.5128	0.51242	5.	0.7	0.64	18.86	18.055	15.65	15.608	38.93	38.675
VRT_D1	0.704	0.703	0.5127	0.51241	5.	0.7	0.66	19.84	13.950	15.67	15.359	39.72	39.192
VRT_D1	0.704	0.704	0.5127	0.51241	5.	0.7	0.66	21.21	10.446	15.75	15.168	41.19	40.152
VRT_D1	0.705	0.704	0.5127	0.51231	3.	1.1	0.82	18.84	17.555	15.61	15.555	38.93	40.871
VRT_D/	0.749	0.700	0.5119	0.51169	-	1.6	1.77	18.57	18.283	15.71	15.695	39.23	38.149
VRT_D1	0.704	0.704	0.5127	0.51237	4.	0.8	0.72	18.70	16.214	15.64	15.511	38.84	38.598
VRT_D2	0.706	0.706	0.5127	0.51236	4.	0.9	0.74	20.94	18.763	15.70	15.583	40.03	38.150
JG-9	0.704	0.703	0.5127	0.51235	4.	0.9	0.75	19.07	14.426	15.60	15.373	39.09	38.528
JG-13	0.705	0.705	0.5127	0.51240	5.	0.7	0.67	18.97	15.416	15.64	15.447	38.96	38.699
JG-260	0.705	0.704	0.5128	0.51243	5.	0.7	0.64	18.79	15.776	15.60	15.437	38.67	38.380
ZB-443	0.704	0.703	0.5128	0.51243	5.	0.7	0.62	19.25	15.769	15.63	15.446	38.98	38.637
BCR-2	0.705		0.5126										
RGM-2	0.704		0.5127										
BHVO-2								18.59		15.53		38.18	
BE-N								19.18		15.59		38.99	

Uncertainties for Sr and Nd isotope values are given as 2 se, those for Pb isotope values are reported as 2sd; the uncertainties correspond to the last or last two digits. An age of 387 Ma was used for recalculation to initial values.

Author statement

Václav Kachlík: Conceptualization, Investigation, Data acquisition, Writing. Vladislav Rapprich: Conceptualization, Investigation, Writing. John M. Hora: Conceptualization, Investigation, Writing. Tomáš Magna: Conceptualization, Investigation, Data acquisition, Writing, Funding acquisition. O. Krentz: Investigation, Writing. Q. Crowley: Investigation, Data acquisition, Writing. Ondřej Pour: Investigation, Data acquisition. Zuzana Čvančarová: Data acquisition.

Declaration of interests

☒ The authors declare that they have no known competing financial interests or personal relationships that could have appeared to influence the work reported in this paper.

☐ The authors declare the following financial interests/personal relationships which may be considered as potential competing interests:

Late Early Devonian to Middle Devonian (~ 400-370 Ma)

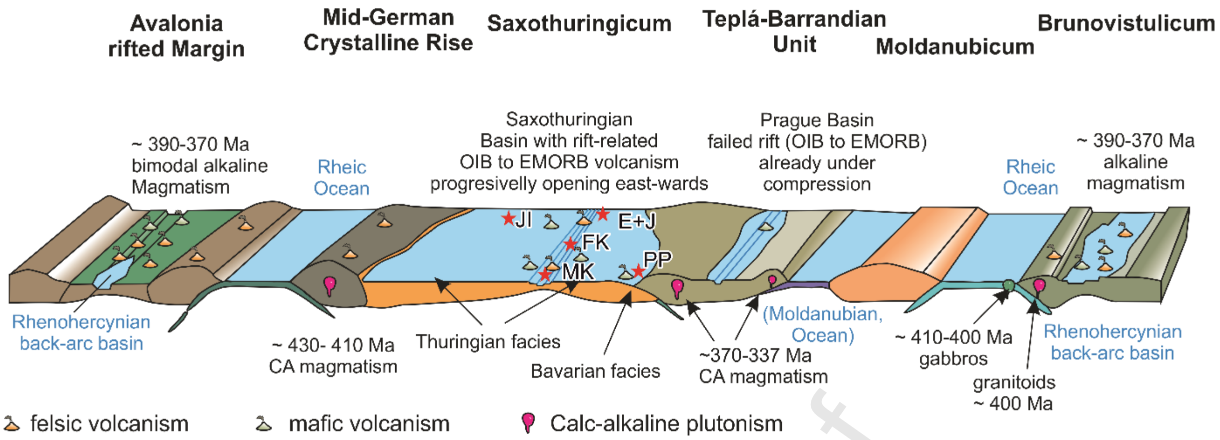

Research highlights

- Existing data for peri-Gondwana reveals three intracontinental rifting episodes
- Recurrent Cambrian– early Carboniferous bimodal felsic and mafic OIB to MORB-like magmatism
- Conclusive evidence for widespread basaltic volcanism along N Gondwana margin
- Long-duration episodic rifting along northern Gondwana is linked to plume activity
- More developed rifting in W Saxothuringian and progressive W-to-E rift propagation